Acknowledgments

Daiichi-Sankyo Co. Ltd. (Tokyo, Japan), APEX Co., Ltd. (Nagoya, Japan), Suzuken Memorial Foundation, and Japan Society for the Promotion of Science (Grant no. 26461074) supported this work.

References

[1] The Antiarrhythmics versus Implantable Defibrillators (AVID) Investigators. A comparison of antiarrhythmic-drug therapy with implantable defibrillators in patients resuscitated from near-fatal ventricular arrhythmias. New Engl J Med 1997;337:1576–83.
[2] Connolly SJ, Hallstrom AP, Cappato R, et al. Meta-analysis of the implantable cardioverter defibrillator secondary prevention trials. AVID, CASH and CIDS studies. Antiarrhythmics vs Implantable Defibrillator study. Cardiac Arrest Study Hamburg. Canadian Implantable Defibrillator Study. Eur Heart J 2000;21:2071–8.
[3] Moss AJ, Zareba W, Hall WJ, et al. Prophylactic implantation of a defibrillator in patients with myocardial infarction and reduced ejection fraction. New Engl J Med 2002;346:877–83.
[4] Bardy GH, Lee KL, Mark DB, et al. Amiodarone or an implantable cardioverter-defibrillator for congestive heart failure. New Engl J Med 2005;352:225–37.
[5] Moss AJ, Greenberg H, Case RB, et al. Long-term clinical course of patients after termination of ventricular tachyarrhythmia by an implanted defibrillator. Circulation 2004;110:3760–5.
[6] Poole JE, Johnson GW, Hellkamp AS, et al. Prognostic importance of defibrillator shocks in patients with heart failure. New Engl J Med 2008;359:1009–17.
[7] Huang DT, Traub D. Recurrent ventricular arrhythmia storms in the age of implantable cardioverter defibrillator therapy: a comprehensive review. Prog Cardiovasc Dis 2008;51:229–36.
[8] Exner DV, Pinski SL, Wyse DG, et al. Electrical storm presages nonsudden death: the antiarrhythmics versus implantable defibrillators (AVID) trial. Circulation 2001;103:2066–71.
[9] Sesselberg HW, Moss AJ, McNitt S, et al. Ventricular arrhythmia storms in postinfarction patients with implantable defibrillators for primary prevention indications: a MADIT-II substudy. Heart Rhythm 2007;4:1395–402.
[10] Goldenberg I, Moss AJ, Hall WJ, et al. Causes and consequences of heart failure after prophylactic implantation of a defibrillator in the multicenter automatic defibrillator implantation trial II. Circulation 2006;113:2810–7.
[11] Nayyar S, Ganesan AN, Brooks AG, et al. Venturing into ventricular arrhythmia storm: a systematic review and meta-analysis. Eur Heart J 2013;34:560–71.
[12] Sweeney MO, Sherfesee L, DeGroot PJ, Wathen MS, Wilkoff BL. Differences in effects of electrical therapy type for ventricular arrhythmias on mortality in implantable cardioverter-defibrillator patients. Heart Rhythm 2010;7:353–60.
[13] Stempniewicz P, Cheng A, Connolly A, et al. Appropriate and inappropriate electrical therapies delivered by an implantable cardioverter-defibrillator: effect on intracardiac electrogram. J Cardiovasc Electrophysiol 2011;22:554–60.
[14] Tsuji Y, Hojo M, Voigt N, et al. Ca^{2+}-related signaling and protein phosphorylation abnormalities play central roles in a new experimental model of electrical storm. Circulation 2011;123:2192–203.
[15] Dorian P, Hohnloser SH, Thorpe KE, et al. Mechanisms underlying the lack of effect of implantable cardioverter-defibrillator therapy on mortality in high-risk patients with recent myocardial infarction: insights from the Defibrillation in Acute Myocardial Infarction Trial (DINAMIT). Circulation 2010;122:2645–52.
[16] Bhavnani SP, Kluger J, Coleman CI, et al. The prognostic impact of shocks for clinical and induced arrhythmias on morbidity and mortality among patients with implantable cardioverter-defibrillators. Heart Rhythm 2010;7:755–60.
[17] Swerdlow C, Ellenbogen KA, Klein GJ. Resolving the conflict: implantable cardioverter-defibrillator shocks for ventricular tachyarrhythmias increase mortality. Heart Rhythm 2012;9:1328–30.
[18] Sweeney MO. Point: implantable cardioverter-defibrillator shocks for ventricular tachyarrhythmias increase mortality. Heart Rhythm 2012;9:985–7.
[19] Dorian P. Counterpoint: implantable cardioverter-defibrillator shocks for ventricular tachyarrhythmias do not increase mortality. Heart Rhythm 2012;9:988–91.
[20] Powell BD, Saxon LA, Boehmer JP, et al. Survival after shock therapy in implantable cardioverter-defibrillator and cardiac resynchronization therapy-defibrillator recipients according to rhythm shocked. The ALTITUDE survival by rhythm study. J Am Coll Cardiol 2013;62:1674–9.
[21] Moss AJ, Schuger C, Beck CA, et al. Reduction in inappropriate therapy and mortality through ICD programming. New Engl J Med 2012;367:2275–83.
[22] Cevik C, Perez-Verdia A, Nugent K. Implantable cardioverter defibrillators and their role in heart failure progression. Europace 2009;11:710–5.
[23] Shepard RK, Ellenbogen KA. Predicting outcome after implantable cardioverter-defibrillator therapy: a new piece to the puzzle? J Am Coll Cardiol 2009;54:829–31.
[24] Nikolski VP, Efimov IR. Electroporation of the heart. Europace 2005;7(Suppl. 2):S146–S154.
[25] Wang YT, Efimov IR, Cheng Y. Electroporation induced by internal defibrillation shock with and without recovery in intact rabbit hearts. Am J Physiol Heart Circ Physiol 2012;303:H439–49.
[26] Tereshchenko LG, Faddis MN, Fetics BJ, et al. Transient local injury current in right ventricular electrogram after implantable cardioverter-defibrillator shock predicts heart failure progression. J Am Coll Cardiol 2009;54:822–8.
[27] Bode F, Wiegand U, Raasch W, Richardt G, Potratz J. Differential effects of defibrillation on systemic and cardiac sympathetic activity. Heart 1998;79:560–7.
[28] Heusch G, Deussen A. The effects of cardiac sympathetic nerve stimulation on perfusion of stenotic coronary arteries in the dog. Circ Res 1983;53:8–15.
[29] Grimm M, Brown JH. β-Adrenergic receptor signaling in the heart: role of CaMKII. J Mol Cell Cardiol 2010;48:322–30.
[30] Fast VG, Cheek ER, Pollard AE, Ideker RE. Effects of electrical shocks on Ca_i^{2+} and V_m in myocyte cultures. Circ Res 2004;94:1589–97.
[31] Zhang R, Khoo MS, Wu Y, et al. Calmodulin kinase II inhibition protects against structural heart disease. Nat Med 2005;11:409–17.
[32] Antos CL, Frey N, Marx SO, et al. Dilated cardiomyopathy and sudden death resulting from constitutive activation of protein kinase a. Circ Res 2001;89:997–1004.
[33] Bolli R, Marban E. Molecular and cellular mechanisms of myocardial stunning. Physiol Rev 1999;79:609–34.
[34] Ling H, Gray CB, Zambon AC, et al. Ca^{2+}/calmodulin-dependent protein kinase IIδ mediates myocardial ischemia/reperfusion injury through nuclear factor-κB. Circ Res 2013;112:935–44.
[35] Koretsune Y, Marban E. Cell calcium in the pathophysiology of ventricular fibrillation and in the pathogenesis of postarrhythmic contractile dysfunction. Circulation 1989;80:369–79.
[36] Zaugg CE, Ziegler A, Lee RJ, Barbosa V, Buser PT. Postresuscitation stunning: postfibrillatory myocardial dysfunction caused by reduced myofilament Ca^{2+} responsiveness after ventricular fibrillation-induced myocyte Ca^{2+} overload. J Cardiovasc Electrophysiol 2002;13:1017–24.
[37] Birnie D, Tung S, Simpson C, et al. Complications associated with defibrillation threshold testing: the Canadian experience. Heart Rhythm 2008;5:387–90.
[38] Wehrens XH, Marks AR. Novel therapeutic approaches for heart failure by normalizing calcium cycling. Nat Rev Drug Discov 2004;3:565–73.
[39] Maier LS, Zhang T, Chen L, et al. Transgenic CaMKIIδ$_C$ overexpression uniquely alters cardiac myocyte Ca^{2+} handling: reduced SR Ca^{2+} load and activated SR Ca^{2+} release. Circ Res 2003;92:904–11.
[40] Zhang T, Maier LS, Dalton ND, et al. The δ_C isoform of CaMKII is activated in cardiac hypertrophy and induces dilated cardiomyopathy and heart failure. Circ Res 2003;92:912–9.
[41] Wu Y, Temple J, Zhang R, et al. Calmodulin kinase II and arrhythmias in a mouse model of cardiac hypertrophy. Circulation 2002;106:1288–93.
[42] Braz JC, Gregory K, Pathak A, et al. PKC-α regulates cardiac contractility and propensity toward heart failure. Nat Med 2004;10:248–54.
[43] Tsuji Y, Opthof T, Yasui K, et al. Ionic mechanisms of acquired QT prolongation and torsades de pointes in rabbits with chronic complete atrioventricular block. Circulation 2002;106:2012–8.
[44] Tsuji Y, Zicha S, Qi XY, Kodama I, Nattel S. Potassium channel subunit remodeling in rabbits exposed to long-term bradycardia or tachycardia: discrete arrhythmogenic consequences related to differential delayed-rectifier changes. Circulation 2006;113:345–55.
[45] Luo M, Anderson ME. Mechanisms of altered Ca^{2+} handling in heart failure. Circ Res 2013;113:690–708.
[46] Erickson JR, Joiner ML, Guan X, et al. A dynamic pathway for calcium-independent activation of CaMKII by methionine oxidation. Cell 2008;133:462–74.
[47] Rokita AG, Anderson ME. New therapeutic targets in cardiology: arrhythmias and Ca^{2+}/calmodulin-dependent kinase II (CaMKII). Circulation 2012;126:2125–39.
[48] Swaminathan PD, Purohit A, Hund TJ, Anderson ME. Calmodulin-dependent protein kinase II: linking heart failure and arrhythmias. Circ Res 2012;110:1661–77.
[49] Luczak ED, Anderson ME. CaMKII oxidative activation and the pathogenesis of cardiac disease. J Mol Cell Cardiol 2014. http://dx.doi.org/10.1016/j.yjmcc.2014.02.004.
[50] Ling H, Zhang T, Pereira L, et al. Requirement for Ca^{2+}/calmodulin-dependent kinase II in the transition from pressure overload-induced cardiac hypertrophy to heart failure in mice. J Clin Invest 2009;119:1230–40.
[51] Anderson ME. CaMKII and a failing strategy for growth in heart. J Clin Invest 2009;119:1082–5.
[52] Odagiri K, Katoh H, Kawashima H, et al. Local control of mitochondrial membrane potential, permeability transition pore and reactive oxygen species by calcium and calmodulin in rat ventricular myocytes. J Mol Cell Cardiol 2009;46:989–97.
[53] Joiner ML, Koval OM, Li J, et al. CaMKII determines mitochondrial stress responses in heart. Nature 2012;491:269–73.
[54] Sossalla S, Fluschnik N, Schotola H, et al. Inhibition of elevated Ca^{2+}/calmodulin-dependent protein kinase II improves contractility in human failing myocardium. Circ Res 2010;107:1150–61.
[55] van Oort RJ, McCauley MD, Dixit SS, et al. Ryanodine receptor phosphorylation by calcium/calmodulin-dependent protein kinase II promotes life-threatening ventricular arrhythmias in mice with heart failure. Circulation 2010;122:2669–79.
[56] Respress JL, van Oort RJ, Li N, et al. Role of RyR2 phosphorylation at S2814 during heart failure progression. Circ Res 2012;110:1474–83.

Please cite this article as: Tsuji Y, et al. Molecular mechanisms of heart failure progression associated with implantable cardioverter-defibrillator shocks for ventricular tachyarrhythmias. J Arrhythmia (2014), http://dx.doi.org/10.1016/j.joa.2014.04.003

[57] Blaich A, Welling A, Fischer S, et al. Facilitation of murine cardiac L-type $Ca_V1.2$ channel is modulated by calmodulin kinase II-dependent phosphorylation of S1512 and S1570. Proc Natl Acad Sci USA 2010;107:10285–9.
[58] Grueter CE, Abiria SA, Dzhura I, et al. L-type Ca^{2+} channel facilitation mediated by phosphorylation of the β subunit by CaMKII. Mol Cell 2006;23: 641–50.
[59] Koval OM, Guan X, Wu Y, et al. $Ca_V1.2$ β-subunit coordinates CaMKII-triggered cardiomyocyte death and afterdepolarizations. Proc Natl Acad Sci USA 2010;107:4996–5000.
[60] Maltsev VA, Reznikov V, Undrovinas NA, Sabbah HN, Undrovinas A. Modulation of late sodium current by Ca^{2+}, calmodulin, and CaMKII in normal and failing dog cardiomyocytes: similarities and differences. Am J Physiol Heart Circ Physiol 2008;294:H1597–608.
[61] Koval OM, Snyder JS, Wolf RM, et al. Ca^{2+}/calmodulin-dependent protein kinase II-based regulation of voltage-gated Na^+ channel in cardiac disease. Circulation 2012;126:2084–94.
[62] Ashpole NM, Herren AW, Ginsburg KS, et al. Ca^{2+}/calmodulin-dependent protein kinase II (CaMKII) regulates cardiac sodium channel $Na_V1.5$ gating by multiple phosphorylation sites. J Biol Chem 2012;287:19856–69.
[63] Yao L, Fan P, Jiang Z, et al. $Na_V1.5$-dependent persistent Na^+ influx activates CaMKII in rat ventricular myocytes and $N_{1325}S$ mice. Am J Physiol Cell Physiol 2011;301:C577–86.
[64] Reiken S, Gaburjakova M, Gaburjakova J, et al. β-Adrenergic receptor blockers restore cardiac calcium release channel (ryanodine receptor) structure and function in heart failure. Circulation 2001;104:2843–8.
[65] Okuda S, Yano M, Doi M, et al. Valsartan restores sarcoplasmic reticulum function with no appreciable effect on resting cardiac function in pacing-induced heart failure. Circulation 2004;109:911–9.
[66] Lehnart SE, Mongillo M, Bellinger A, et al. Leaky Ca^{2+} release channel/ryanodine receptor 2 causes seizures and sudden cardiac death in mice. J Clin Invest 2008;118:2230–45.
[67] Wehrens XH, Lehnart SE, Reiken SR, et al. Protection from cardiac arrhythmia through ryanodine receptor-stabilizing protein calstabin2. Science 2004;304: 292–6.
[68] Kobayashi S, Bannister ML, Gangopadhyay JP, et al. Dantrolene stabilizes domain interactions within the ryanodine receptor. J Biol Chem 2005;280: 6580–7.
[69] Kobayashi S, Yano M, Suetomi T, et al. Dantrolene, a therapeutic agent for malignant hyperthermia, markedly improves the function of failing cardiomyocytes by stabilizing interdomain interactions within the ryanodine receptor. J Am Coll Cardiol 2009;53:1993–2005.
[70] Zhou Q, Xiao J, Jiang D, et al. Carvedilol and its new analogs suppress arrhythmogenic store overload-induced Ca^{2+} release. Nat Med 2011;17:1003–9.
[71] Parikh A, Mantravadi R, Kozhevnikov D, et al. Ranolazine stabilizes cardiac ryanodine receptors: a novel mechanism for the suppression of early afterdepolarization and torsades de pointes in long QT type 2. Heart Rhythm 2012;9:953–60.
[72] Mochizuki M, Yano M, Oda T, et al. Scavenging free radicals by low-dose carvedilol prevents redox-dependent Ca^{2+} leak via stabilization of ryanodine receptor in heart failure. J Am Coll Cardiol 2007;49:1722–32.
[73] Moreno JD, Clancy CE. Pathophysiology of the cardiac late Na current and its potential as a drug target. J Mol Cell Cardiol 2012;52:608–19.

Please cite this article as: Tsuji Y, et al. Molecular mechanisms of heart failure progression associated with implantable cardioverter-defibrillator shocks for ventricular tachyarrhythmias. J Arrhythmia (2014), http://dx.doi.org/10.1016/j.joa.2014.04.003

INTERNAL MEDICINE

□ CASE REPORT □

Multiform Premature Ventricular Contractions and Polymorphic Ventricular Tachycardia Caused by Purkinje Activity with Slow Conduction in Idiopathic Ventricular Fibrillation

Satoshi Nagase, Kimikazu Banba, Nobuhiro Nishii, Hiroshi Morita, Kengo Fukushima Kusano, Tohru Ohe and Hiroshi Ito

Abstract

In several cases with idiopathic ventricular fibrillation (VF), VF was initiated by premature ventricular contractions (PVCs) from the Purkinje system. However, the precise characteristics of the Purkinje activity in patients with idiopathic VF remain unclear. We performed an electrophysiological study in a patient with idiopathic VF and examined the correlation between the Purkinje potential and the incidence of PVCs/polymorphic ventricular tachycardia (PMVT). In this case of idiopathic VF, the Purkinje activity caused multiform PVCs and PMVT. The The Purkinje activity and slow conduction of Purkinje fibers are associated with the occurrence of multiform PVCs and PMVT.

Key words: Purkinje, ventricular fibrillation, polymorphic ventricular tachycardia, premature ventricular contraction, slow conduction

(Intern Med 53: 725-728, 2014)
(DOI: 10.2169/internalmedicine.53.1147)

Introduction

It has been reported that idiopathic ventricular fibrillation (VF) is induced by premature ventricular contractions (PVCs) with very short coupling intervals originating from the Purkinje system (1-4). We performed an electrophysiological study (EPS) in a patient with idiopathic VF and examined the correlation between the Purkinje potential and the incidence of PVCs.

Case Report

A 29-year-old woman was referred to our hospital on account of frequent episodes of VF initiated by PVCs with a short coupling interval and several implantable cardioverter-defibrillator (ICD) discharges (Fig. 1A). The patient had been diagnosed with idiopathic VF at 26 years of age due to the occurrence of spontaneous VF episodes, a normal QT interval and no evidence of Brugada-type electrocardiogram (ECG) findings. Cardiac echocardiography, right and left ventriculography, coronary angiography and a myocardial biopsy demonstrated no abnormalities. An ICD was immediately implanted after diagnosis, and treatment with oral atenolol and disopyramide was initiated.

ECG recordings obtained after admission showed multiform PVCs (Fig. 1B) and non-sustained polymorphic ventricular tachycardia (PMVT). All PVCs had a right bundle branch block configuration with various axis deviations and QRS durations. After obtaining the patient's informed consent, EPS was performed under local anesthesia. A 7-French 20-pole electrode catheter (1-3-1 mm interelectrode spacing; Cordis Webster, Diamond Bar, USA) was positioned at the left ventricular (LV) septum, and a quadripolar electrode catheter was positioned at the bundle of His recording region (Fig. 2A). During EPS, PVCs and non-sustained PMVT were frequently observed. Under a sinus rhythm, serial Purkinje potentials were recorded immediately before the onset of QRS at the LV septum (Fig. 2B). Although the PVCs exhibited multiple configurations, diastolic Purkinje

Departments of Cardiovascular Medicine, Okayama University Graduate School of Medicine, Dentistry, and Pharmaceutical Sciences, Japan
Received for publication June 9, 2013; Accepted for publication October 15, 2013
Correspondence to Dr. Satoshi Nagase, snagase@cc.okayama-u.ac.jp

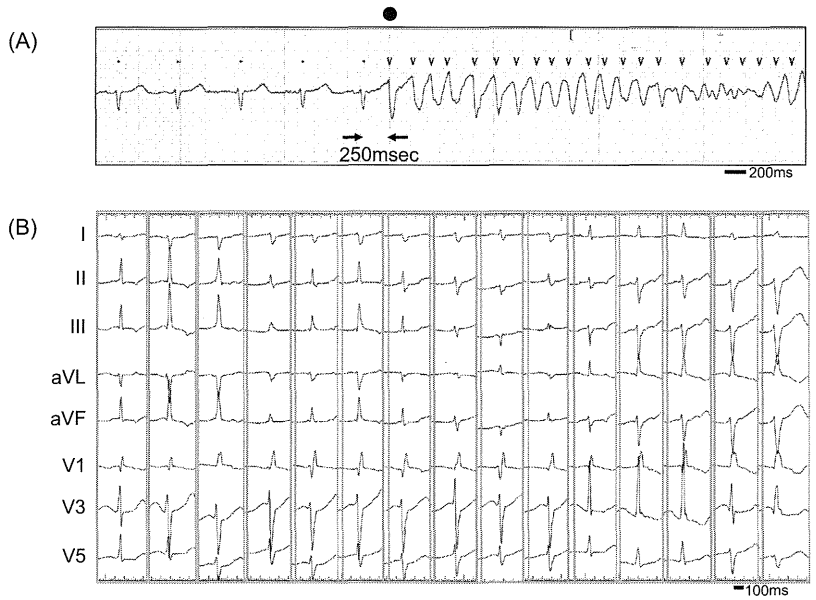

Figure 1. (A) ECG showing PMVT initiated by a PVC (●) with a short coupling interval (250 ms). (B) Surface ECG showing multiform PVCs. All PVCs had a right bundle branch block configuration with various axis deviations and QRS durations.

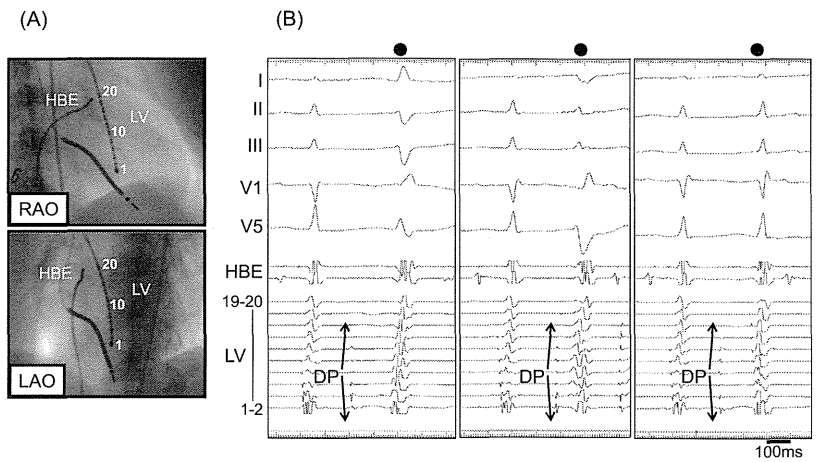

Figure 2. (A) Catheter position. Fluoroscopic right anterior oblique (RAO) and left anterior oblique (LAO) views of the 20-pole electrode catheter positioned at the left ventricular septum (LV) and the quadripolar catheter positioned at the bundle of His region (HBE). (B) Surface ECG and intracardiac electrograms demonstrating multiform PVCs (●) and diastolic Purkinje potentials (DPs; arrow). The configuration of each PVC was different; however, a DP with an identical sequence always preceded each PVC. During sinus rhythm, serial Purkinje potentials were recorded immediately before the onset of QRS.

potentials (DPs) with an identical sequence recorded at the LV septum always preceded each PVC (Fig. 2B, 3A). Occasionally, the DP was blocked, and no PVC appeared (Fig. 3A). The DPs also preceded each QRS complex of PMVT (Fig. 3B).

In order to examine the relationships between the preceding sinus cycle length, DP and multiform PVCs, we measured the QRS duration, H0-H1 interval (which reflects the preceding sinus cycle length), H1-DP interval, H1-QRS interval and DP-QRS interval in each PVC (Fig. 4). We found no relationships between the H0-H1 interval and H1-DP interval (Fig. 4A). However, inverse correlations were found between the H1-DP interval and DP-QRS interval ($r=-0.76$, $p<0.0001$) (Fig. 4C) and between the H1-QRS interval and

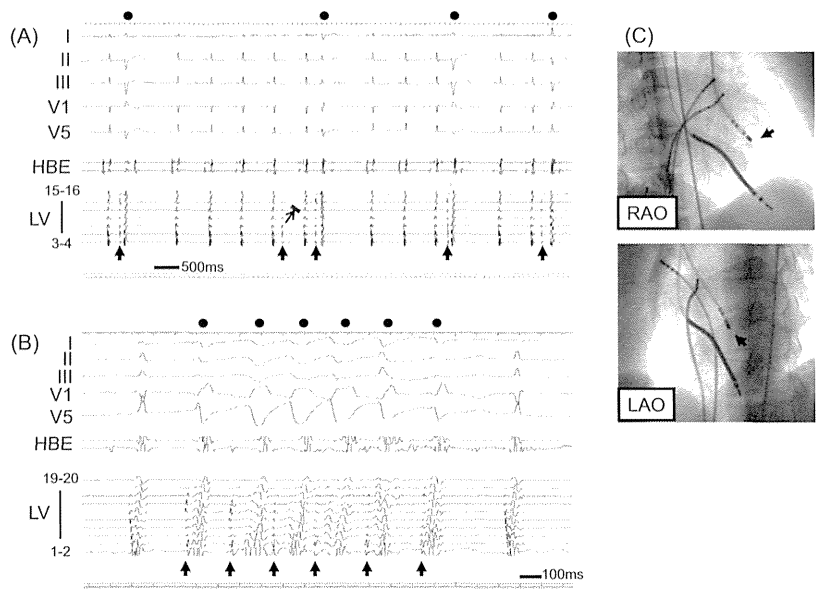

Figure 3. **(A) Surface ECG and intracardiac electrograms demonstrating multiform PVCs (●) and DPs (arrow). The second DP was blocked. (B) Surface ECG and intracardiac electrograms demonstrating a 6-beat run of non-sustained PMVT (●). A Purkinje potential (arrow) preceded each QRS complex of PMVT. Widening of the ventricular activity was observed on the second and fourth beats of NSVT. This finding possibly represents a conduction delay in the myocardium. (C) Catheter position. Fluoroscopic RAO and LAO views of the ablation catheter (arrow) positioned at the left ventricular septum.**

QRS duration of the PVCs (r=-0.80, p<0.0001) (Fig. 4D). Only very short H1-QRS intervals caused 4- to 6-beat PMVT runs.

The PVCs and non-sustained PMVT were completely eliminated following radiofrequency (RF) catheter ablation at the recording sites of the DPs in the mid-LV septum (Fig. 3C). A total of 14 RF applications were delivered to the area with the earliest DP and around the earliest DP site in which a DP was recorded. During the follow-up period of 96 months, three episodes of ICD discharge were recorded. However, after the administration of oral atenolol and disopyramide, no ICD discharges were observed.

Discussion

In some cases of idiopathic VF, specific PVCs with a very short coupling interval induce PMVT and VF; catheter ablation to treat the PVCs originating from Purkinje fibers can be used to eliminate this type of idiopathic VF (1-5). However, the precise characteristics of arrhythmogenic Purkinje activation have not been described in previous reports.

In the present case, we were able to record frequent episodes of abnormal activation of the Purkinje fiber during EPS; therefore, it was possible to determine the precise characteristics of the abnormal Purkinje activation and examine the relationship between Purkinje activation and the incidence of PVCs. The results of this study are as follows: [1] activation of the Purkinje fiber caused multiform PVCs and PMVT; [2] slow conduction was observed in the Purkinje fiber and/or Purkinje-muscle junction; [3] the incidence of PVCs with a very short coupling interval was associated with a longer QRS duration following non-sustained PMVT. The Purkinje activation was independent of the preceding normal sinus activation, as no relationships were found between the preceding sinus cycle length (H0-H1) and the H1-DP interval. Accordingly, activation of the Purkinje fiber is associated with automaticity, and the H1-DP interval is variable.

The occurrence of multiform PVCs with various QRS durations is associated with the alteration of multiple exits and variability of the refractory period in the Purkinje network and Purkinje-muscle junction. The variable sequence of local LV electrograms observed in each PVC may also represent the alteration of exit sites and dispersion of refractoriness in the Purkinje network and Purkinje-muscle junction (Fig. 2B). Because the exit sites were not uniform, we were unable to determine the properties of the decremental conduction from the DP to the exit site. However, due to the prolonged DP-QRS interval, a conduction delay between the abnormal Purkinje activity and the exit site may have been present in this patient.

The DP, a trigger of PMVT of more than a four-beat run, exhibited a very short H1-QRS interval and an extremely long QRS duration of the initial ventricular ectopic beat (Fig. 4D). We speculate that the PVCs with a remarkably short coupling interval were accompanied by heterogeneity

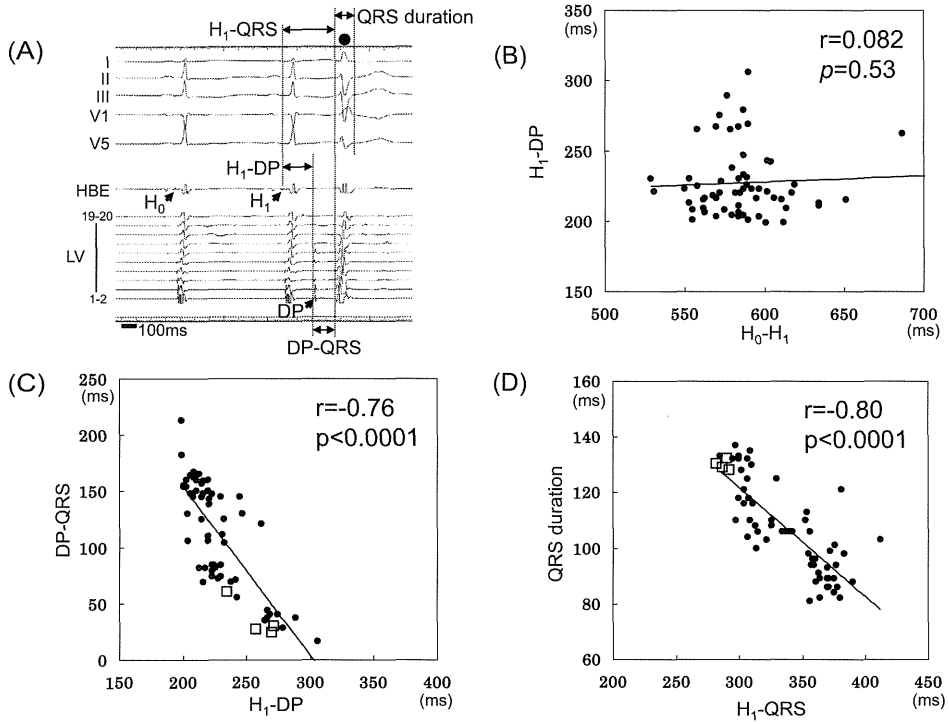

Figure 4. (A) Measurement parameters on EPS. ● Indicates a PVC. (B) Relationship between the H0-H1 and H1-DP intervals. No relationships were found between the two parameters. This finding suggests that the Purkinje activation was independent of the preceding normal sinus activation. (C) Relationship between the H1-DP and DP-QRS intervals. An inverse relationship was observed (r= –0.76, p<0.0001). □ Indicates a non-sustained PMVT run with more than four beats. (D) Relationship between the H1-QRS interval and QRS duration of the PVCs. An inverse relationship was observed (r=–0.80, p<0.0001). □ Indicates a non-sustained PMVT run with more than four beats. Only very short H-QRS intervals caused 4- to 6-beat PMVT runs.

and dispersion of refractoriness in the Purkinje network or Purkinje-muscle junction, which may have caused reentrant activity. However, we cannot deny the possibility that focal rapid activity in the Purkinje network caused the PMVT. In any case, the Purkinje network may play an important role in both the initiation and perpetuation of PMVT and subsequent VF.

In this case of idiopathic VF, the Purkinje activity in the LV caused multiform PVCs and PMVT. Abnormal Purkinje activity and slow conduction of the Purkinje fiber and/or the Purkinje-muscle junction were observed in this patient.

The authors state that they have no Conflict of Interest (COI).

References

1. Haïssaguerre M, Shah DC, Jaïs P, et al. Role of Purkinje conducting system in triggering of idiopathic ventricular fibrillation. Lancet **359**: 677-678, 2002.
2. Haïssaguerre M, Shoda M, Jaïs P, et al. Mapping and ablation of idiopathic ventricular fibrillation. Circulation **106**: 962-967, 2002.
3. Nogami A, Sugiyasu A, Kubota S, Kato K. Mapping and ablation of idiopathic ventricular fibrillation from the Purkinje system. Heart Rhythm **2**: 646-649, 2005.
4. Tsuchiya T, Nakagawa S, Yanagita Y, Fukunaga T. Transition from purkinje fiber-related rapid polymorphic ventricular tachycardia to sustained monomorphic ventricular tachycardia in a patient with a structurally normal heart: a case report. J Cardiovasc Electrophysiol **18**: 102-105, 2007.
5. Leenhardt A, Glaser E, Burguera M, et al. Short-coupled variant of torsade de pointes. A new electrocardiographic entity in the spectrum of idiopathic ventricular tachyarrhythmias. Circulation **89**: 206-215, 1994.

Nonsense-mediated mRNA decay due to a *CACNA1C* splicing mutation in a patient with Brugada syndrome

Megumi Fukuyama, MD,* Seiko Ohno, MD, PhD,* Qi Wang, BSc,* Takeshi Shirayama, MD, PhD,† Hideki Itoh, MD, PhD,* Minoru Horie, MD, PhD*

*From the *Department of Cardiovascular and Respiratory Medicine, Shiga University of Medical Science, Shiga, Japan and †Division of Cardiovascular Medicine, Kyoto Prefectural University of Medicine, Kyoto, Japan.*

BACKGROUND Brugada syndrome (BrS) is an inherited cardiac arrhythmia associated with sudden death due to ventricular fibrillation. Mutations in genes related to the cardiac L-type calcium channel have been reported to be causative of BrS. Generally, the messenger RNA (mRNA) that contains a nonsense mutation is rapidly degraded via its decay pathway, which is known as nonsense-mediated mRNA decay (NMD). Previously, we reported a male patient with BrS who carried c.1896G > A (the first nucleotide of *CACNA1C* exon 14), which caused a synonymous mutation, p.R632R.

OBJECTIVE To examine how the synonymous *CACNA1C* mutation p.R632R produces the phenotype of BrS, with a special emphasis on the splicing error and NMD processes.

METHODS We extracted mRNA from leukocytes of the proband and his 2 children and performed reverse transcription polymerase chain reaction. Complementary DNAs were checked by using direct sequencing and quantitative analysis.

RESULTS The subsequent sequence electropherogram of the complementary DNAs did not show the substitution of the nucleotide identified in the genomic DNA of the proband. In the mRNA quantification analysis, we confirmed that reduction in the *CACNA1C* expression level was suspected to be caused by NMD.

CONCLUSIONS Mutant mRNA with a c.1896G > A substitution may be diminished by NMD, and the resultant decrease in *CACNA1C* message leads to a novel mechanism for inducing BrS that is distinct from that reported previously.

KEYWORDS L-type calcium channel; *CACNA1C*; Nonsense-mediated mRNA decay; Brugada syndrome

ABBREVIATIONS **BrS** = Brugada syndrome; **cDNA** = complementary DNA; **ECG** = electrocardiogram; **HEK** = human embryo kidney; **hERG** = human ether-à-go-go-related gene; $\mathbf{I_{Ca}}$ = calcium current; **ICD** = implantable cardioverter-defibrillator; **mRNA** = messenger RNA; **NMD** = nonsense-mediated mRNA decay; **PCR** = polymerase chain reaction; **PTC** = premature termination codon; **qPCR** = quantitative polymerase chain reaction; **RT-PCR** = reverse transcription polymerase chain reaction; **VF** = ventricular fibrillation

(Heart Rhythm 2014;11:629–634)

Introduction

Brugada syndrome (BrS) is an inherited cardiac arrhythmia associated with sudden death due to ventricular fibrillation (VF).[1] The diagnosis of BrS is based on the presence of ST-segment elevation in the right precordial leads on an electrocardiogram (ECG).[2] Mutations in the *SCN5A*-encoded α subunit of the cardiac sodium channel (Nav1.5) are the most common genetic substrates for BrS.[3] In addition, mutations in genes encoding the cardiac L-type calcium channel (LTCC) account for 10%–15% of BrS cases.[4] The LTCC is composed of 4 subunits: the α_1 subunit encoded by *CACNA1C*, the β_2 subunit encoded by *CACNB2b*, and the $\alpha_2\delta$ subunits encoded by *CACNA2D1*.

In general, nonsense mutations are known to produce some form of genetic disease: a nonsense mutation converts an amino acid codon into a termination codon. This causes the protein to be shortened because of the stop codon interrupting its normal code. Messenger RNAs (mRNAs) that contain this type of mutation are rapidly degraded by a decay pathway, a process known as nonsense-mediated mRNA decay (NMD). Abnormally spliced mRNAs are also excluded by an NMD mechanism, and the NMD pathway depends on pre-mRNA splicing at the ribosome. Recently, the NMD process has been suggested to play a more general and evolutionarily important role in the control of overall gene expression as well as in pathological conditions.[5] For example, in long QT syndrome, NMD has been reported in the human ether-à-go-go–related gene (hERG)[6] and splicing

This study was supported, in part, by a Grant-in-Aid for Scientific Research from the Japan Society for the Promotion of Science (KAKENHI) (to Dr Ohno and Dr Horie) and by a Translational Research grant from the Japanese Circulation Society (to Dr Horie). **Address reprint requests and correspondence:** Dr Minoru Horie, Department of Cardiovascular and Respiratory Medicine, Shiga University of Medical Science, Seta-Tsukinowa, Otsu, Shiga 520-2192, Japan. E-mail address: horie@belle.shiga-med.ac.jp.

1547-5271/$-see front matter http://dx.doi.org/10.1016/j.hrthm.2013.12.011

errors usually result in the skipping of exon(s), which in turn produces a frameshift of hERG and, consequently, a premature termination codon (PTC). This mechanism underlies various pathological conditions and modulates their clinical severity.[7,8]

In our previous study,[9] we screened 312 probands with various fatal arrhythmias and identified 6 *CACNA1C* mutations in 7 unrelated probands. These mutations included one synonymous mutation that may cause a splicing error at the mRNA level. The present study aimed to examine the pathological effects of this synonymous *CACNA1C* mutation, with a special emphasis on the splicing error and NMD processes.

Methods

Index patient

The study cohort consisted of 312 probands registered in 2 Japanese institutes—the Shiga University of Medical Science and the Kyoto University Graduate School of Medicine—between 1996 and 2012. All individuals gave written informed consent in accordance with the guidelines approved by the institutional review board of each institute. There were 213 (68.2%) cases of BrS, 39 (12.5%) idiopathic VF, 10 (3.2%) short QT syndrome , 23 (7.4%) BrS + short QT syndrome, and 27 (8.7%) early repolarization syndrome. We screened *CACNA1C*, *CACNB2b*, *SCN5A*, *KCNQ1*, *KCNH2*, *KCNE1-3*, *KCNE5*, *SCN3B*, *SCN4B*, and *KCNJ8* genes by using high-resolution melting analysis or denaturing high-performance liquid chromatography (WAVE system Model 3500, Transgenomic, Omaha, NE) and direct sequencing. High-resolution melting analyses were performed with a LightCycler 480 device (Roche Applied Science, Roche Diagnostic GmbH, Mannheim, Germany). We identified 5 *CACNA1C* mutations including synonymous mutation that may cause splice error in BrS probands.[9] A 38-year-old man with BrS was identified as a carrier of a heterozygous synonymous mutation (p.R632R) caused by a substitution of G with A at codon 1896 (the initial nucleotide of exon 14).[9]

RNA extraction and real-time reverse transcription polymerase chain reaction

In order to clarify the pathological mechanism associated with the induction of BrS phenotypes, we extracted the patients' total RNA from leukocytes in fresh blood by using QIAamp RNA Blood Mini Kits (Qiagen, Valencia, CA). Subsequently, DNase-treated total RNA was reverse transcribed with the SuperScript III First-Strand Synthesis System (Invitrogen, Carlsbad, CA) and was used as a template for the subsequent polymerase chain reaction (PCR). The primer pairs 1F-50R, 12F-15R, 13F-15R, and 14F-16R were used to amplify *CACNA1C* complementary DNA (cDNA). Band sizes were estimated on agarose gels. The products obtained through the reverse transcription polymerase chain reaction (RT-PCR) were then checked by direct sequencing with an ABI PRISM 3130 sequencer (Applied Biosystems, Foster City, CA).

Advanced relative quantification

Relative quantification compares the levels of 2 different genes in a single sample. The first gene was set as the target gene, and the second was used as a reference gene. Dividing the concentration of the target gene by that of the reference gene in the same sample enables the determination of the quantitative difference resulting from RNA degradation. The relative quantification analysis compares 2 different sample ratios, and the final result is expressed as a normalized ratio:

$$\text{Normalized ratio} = \left(\frac{\text{Target concentration}}{\text{Reference concentration}}\right)_{\text{patient}} : \left(\frac{\text{Target concentration}}{\text{Reference concentration}}\right)_{\text{control}}$$

To evaluate the mRNA expression level, we performed quantitative PCR (qPCR) by using a LightCycler 480 Probes Master mix (Roche Diagnostic GmbH, Mannheim, Germany). All qPCRs were performed with a LightCycler 480 device by using the TaqMan method. Data were analyzed by using the $\Delta\Delta C_T$ method. Three healthy human mRNAs were used as control samples. The probe-primer pair *CACNA1C* exon 14F-14R was used as the target gene and *KCNQ1* exon 16F-16R as the reference gene; the primer pairs were designed in accordance with the Universal Probe Library Assay Design Center (https://www.roche-applied-science.com/).

Construction of minigenes

Genomic DNAs from the mutation carrier were used as a template for the PCR amplification of fragments spanning *CACNA1C* exons 14 and 15, including introns 13 to 15. The minigenes were then subcloned into a pSPL3 vector (Invitrogen) and verified by DNA sequencing.

The minigenes in the pSPL3 vector (1 μg) were stably transfected into HEK293 (human embryo kidney 293) cells by using 6 μL of Fugene6 (Roche Diagnostics, Pittsburgh, PA). Forty-eight hours after transfection, we extracted mRNA from the HEK293 cells and performed RT-PCR by using the same protocols as those used for the leukocytes (described above). After RT-PCR, we performed PCR by using the SD6 primer as the forward primer and the SA2 primer as the reverse primer. PCR products were run on agarose gels and checked by direct sequencing.

All the primer sequences used in these experiments are listed in Table 1.

Results

Clinical characteristics of the proband

Figure 1A depicts the 12-lead ECG of the index patient, showing a coved-type ST-segment elevation in lead V_1 and corrected QT interval was within the normal range (383 ms). At the age of 27 years, the patient was hospitalized because of a sudden loss of consciousness after dinner (8 PM). An automated external defibrillator recorded recurrent VF attacks. His cardiac catheterization and echocardiogram

Table 1 Primer sequences

PCR of cDNA from the patient's leukocytes	
1F	5′-ATGCGACCATCTCCACAGTC-3′
12F	5′-GCCGCAGTCAAGTCTAATGTC-3′
13F	5′-GCAGAGATGCTCCTGAAGATG-3′
14F	5′-TACTGGAACTCCTTGAGCAACC-3′
15R	5′-CATCATCCTCTTCATCTGTGG-3′
16R	5′-CTCACATCTGCCCAAAAGGA-3′
50R	5′-GCCTGCGACATGACCATAGA-3′
Quantitative analysis	
14F	5′-TTCAGCTCTAACAACAGGTGTTTC-3′
14R	5′-GTCCAGCACACCTCCTTCAG-3′
KCNQ1-16F	5′-GCTCCCTCACTCTCAGGAAAT-3′
KCNQ1-16R	5′-AGACTGCTCCTGAGCCCC-3′
Minigene analysis	
14F	5′-CTCTGAGAACCTGCAGTGGG-3′
15R	5′-GTTCTAGGCTGGGTGGTGTG-3′
pSPL3-SD6	5′-TCTGAGTCACCTGGACAACC-3′
pSPL3-SA2	5′-ATCTCAGTGGTATTTGTGAGC-3′

F = forward; R = reverse.

findings were normal (ejection fraction, 68%), and a signal-averaged ECG showed a positive late potential (filtered QRS duration, 132 ms; root mean square voltage in the last 40 ms, 15 μV; low-amplitude [<40 μV] signal duration, 45 ms). A cardiac electrophysiological study indicated that double extra stimuli from the right ventricular outflow induced reproducible VF. The patient subsequently received an implantable cardioverter-defibrillator (ICD). Seven years after the implantation, he (at that time 34 years old) suffered a VF attack at night (9 PM), which lasted for 10 seconds but stopped spontaneously (while the ICD was charging).

Genetic testing for *CACNA1C*

As previously reported, DNA sequencing of the patient confirmed a G to A transition at codon 1896 (heterozygous p.R632R) (Figure 1B); the variants were absent in 600 reference alleles obtained from 300 healthy Japanese individuals.[9] This variant does not produce any amino acid changes, but codon 1896 is the initial nucleotide of exon 14 (Figure 1B) and arginine at 632 is highly conserved among multiple species (Figure 1C). We therefore suspected that this synonymous mutation may cause a splicing error that led to the loss of the acceptor site and, consequently, a shorter mRNA with a premature stop codon.

Screening of the patient's family members (Figure 1D) revealed that his *CACNA1C* mutation was inherited by his asymptomatic daughter (age, 13 years), who showed no sign of BrS on ECG. His son was negative for this mutation. The mutation is located in the fourth transmembrane segment of the second domain (DII-S4) of the calcium channel α subunit (not shown). We considered that it may have caused exon skipping because of a splicing error; therefore, we tried to clarify how it affected splicing at the level of the mRNA.

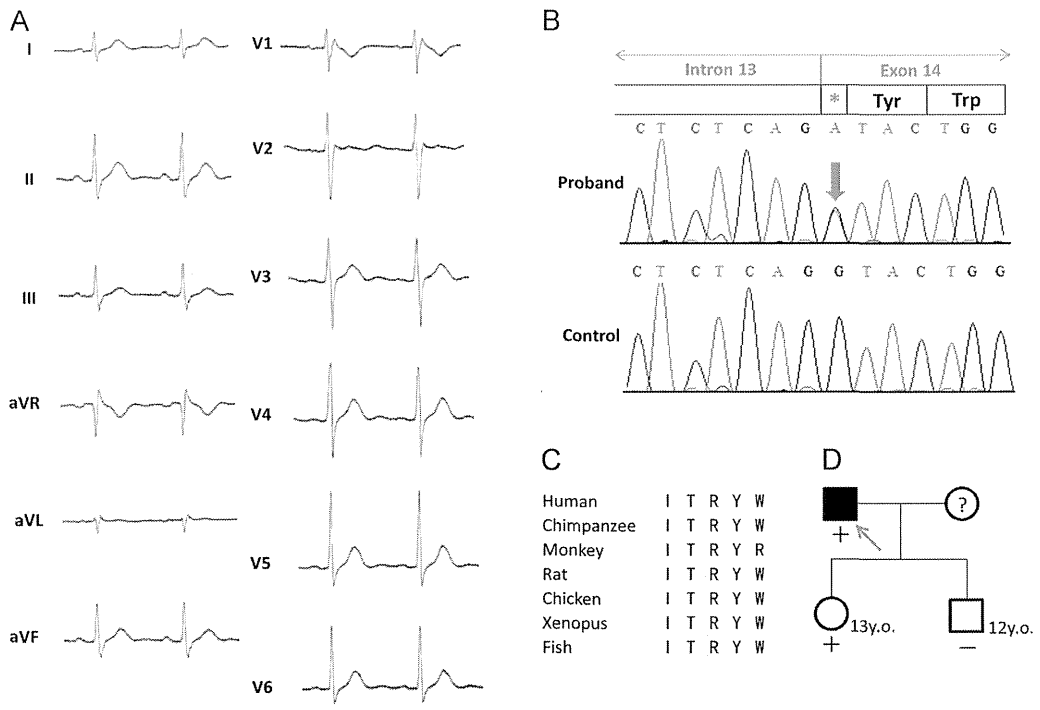

Figure 1 Patient characteristics. **A:** Twelve-lead electrocardiogram showing coved-type ST elevation in lead V_1. **B:** Electropherogram of the mutant *CACNA1C* gene (upper) and the control (lower) showing the heterozygous transition c.1896 G > A (indicated by the asterisk) in the first nucleotide of *CACNA1C* exon 14. **C:** Amino acid sequence alignment showing that arginine at position 632 is highly conserved among multiple species. **D:** Pedigrees of the R632R family. Squares indicate men; circles indicate women; solid symbols indicate phenotype positive; open symbols indicate phenotype negative; question marks indicate no available data; and the arrow indicates the proband. + = genotype positive; − = genotype negative.

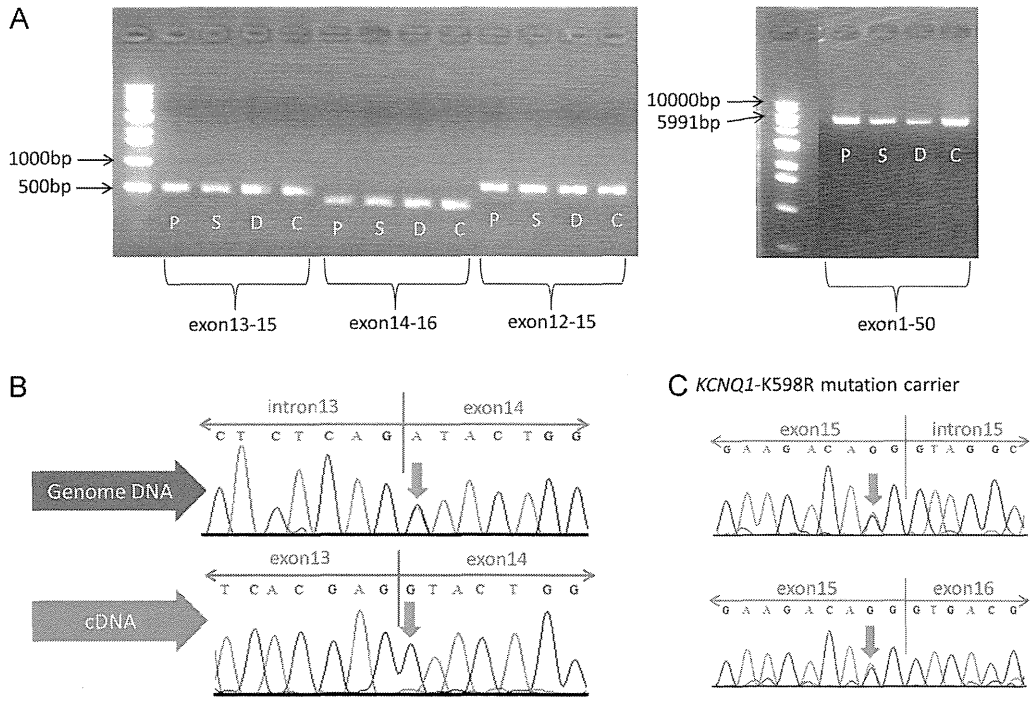

Figure 2 Reverse transcription polymerase chain reaction results. **A:** Agarose gel electrophoresis. P indicates the proband; S indicates his son; D indicates his daughter; and C indicates the control sample (lanes from left to right). 13F-15R: 550 bp; 14F-16R: 440 bp; 12F-15R: 710 bp; 1F-50R: 6000 bp. **B:** Electropherogram of the proband's genomic DNA (upper) and complementary DNA (cDNA; lower). Pink arrows indicate the site of the mutation. The genomic DNA included a heterozygous substitution at the codon, but this substitution was not found in the cDNA. **C:** Electropherogram of the *KCNQ1*-K598R mutation carrier. Both the genomic DNA and the cDNA showed the heterozygous mutation.

RT-PCR and direct sequencing

We therefore examined *CACNA1C* mRNA transcripts freshly isolated from lymphocytes of the index patient, his daughter, and his son. As shown in Figure 2A, RT-PCR was used to evaluate the cDNA products with 4 sets of primer pairs described in the Methods section. The 1F-50R product was estimated to be approximately 6000 bps, the 12F-15R product 710 bps, the 13F-15R product 550 bps, and the 14F-16R product 440 bps. The positions of the band were consistent with the estimated cDNA sizes, and there were no differences among the 2 mutation carriers, the mutation-negative son, and the control. Furthermore, unlike previous reports, only single band was detected in every individual.[7,8]

The patient's genomic DNA sequenced directly (Figure 2B, upper panel) showed clear inclusion of a heterozygous mutation, c.1896G>A (indicated by a red arrow). In contrast, no mutation was found in any of the RT-PCR products from the mutation carriers (lower panel indicated by a red arrow). As to the positive control, we also checked the mRNA of a carrier of the *KCNQ1*-K598R mutation (Figure 2C) and this carrier had a heterozygous mutation in both the genomic DNA and the cDNA. Taken together, the patient's mRNA containing the mutation may have disappeared because of the NMD process.

Quantitative analysis of *CACNA1C* exon 14

To confirm the NMD-dependent elimination of the mutant mRNA, we then conducted a quantitative RT-PCR analysis. Table 2 shows detailed results of advanced relative quantification. Normalized ratios were obtained by dividing "target/reference ratio" of the patients with those of 3 normal controls as described in the Methods. Normalized ratios thus measured in the proband and his daughter (Table 2) were divided by that of his son (noncarrier) and are plotted as bar

Table 2 Values of normalized ratio

		Proband	Daughter	Son
	Target/reference ratio	***4.4***	***5.5***	***7.9***
Control 1	***11.2***	0.39	0.49	0.70
Control 2	***11.5***	0.38	0.48	0.68
Control 3	***12.3***	0.35	0.44	0.64
Mean normalized ratio, mean ± SD		0.37 ± 0.02	0.47 ± 0.02	0.67 ± 0.03

Values in bold italic represent "target/reference ratio" (values of target concentration/reference concentration). Normalized ratios were obtained by dividing bold italic values of the patients with that of normal controls.

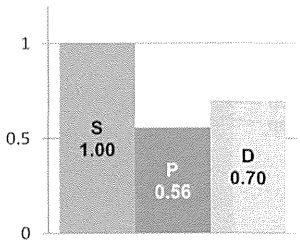

Figure 3 Messenger RNA (mRNA) decrease among the proband and his family as determined by quantitative polymerase chain reaction. P indicates the proband; S indicates his son; and D indicates his daughter. The amount of mutant mRNA was expressed as a percentage of the mRNA of the individual who did not carry the mutation, namely, the son. Compared with his son's mRNA, the proband's mRNA was decreased by 44% while his daughter's mRNA was decreased by 30%.

graphs in Figure 3. Compared to the mutation-negative son (blue bar), mRNA expression levels were significantly reduced in 2 mutation carriers (by 44% and 30%; red and yellow bars, respectively).

Minigene analysis

In the minigene experiments, we also performed RT-PCR and checked cDNAs by using direct sequencing. The control products were expected to be approximately 600 bp in size, but the resulting band positions were estimated to cover over 700 bps in both the mutant and wild-type alleles (Supplemental Figure 1A). We confirmed the sequences of cDNAs and found that *CACNA1C* exon 14 was not skipped in the mutant minigene and that the splice site of exon 15 in the minigenes was different from that seen in the cDNA derived from the patient's leukocytes (Supplemental Figure 1B, left). The first part of exon 15 was skipped (56 bp), and the first part of intron 15 was recognized as exon 15 beyond the boundary of intron 15 and exon 15 (206 bp; Supplemental Figure 1B, right). We therefore concluded that the minigene system we used may not be suitable for reproducing the exon skipping in our patient.

Discussion

In our proband, who presented with symptomatic BrS, we identified a heterozygous substitution of the nucleotide guanine with adenine at codon 1896, which did not cause any change in the residue at codon 632. However, this substitution in the first nucleotide of *CACNA1C* at exon 14 is thought to cause significant alterations during the splicing process between exons 13 and 14. The patient's genomic DNA clearly showed a heterozygous mutation, but the variation was absent at the mRNA level (Figure 2B). Furthermore, the qPCR findings revealed a significant decrease in the patient's normal mRNA level (Figure 3).

As schematically illustrated in Figure 4, the most straightforward explanation for these results is that the splicing error resulted in an exon skipping event and, eventually, a frameshift and PTC, which in turn caused NMD. As per the real-time RT-PCR results, the NMD process decreased the mRNA level in the proband to half that in the mutation-negative son whereas it decreased the mRNA level in the mutation-positive daughter to approximately 70% that in the son (Figure 3). Eventually, the decrease in the mRNA level may lead to the loss of function of the LTCC and, consequently, the BrS phenotype.

The NMD process is an important mechanism because it not only functions as a means of quality control but also modulates the levels of various naturally occurring transcripts, thereby preventing the synthesis of truncated and potentially harmful proteins. Gong et al[6] reported that hERG mutations producing a PTC caused a haploinsufficient type of loss of function in type 2 long QT syndrome via NMD. They described a nonsense mutation in hERG that resulted in mutant mRNA with a PTC. No incomplete mRNA was detected, and quantitative analysis showed that levels of the mutant mRNA, including the PTC, were significantly decreased. In addition, *KCNQ1*-A344Aspl, a mutation in the last nucleotide of exon 7,[7,8] has been shown to induce exon skipping by inhibiting the normal splicing process.

In our study, we hypothesized that the *CACNA1C* splicing mutation would induce NMD and loss of function of the LTCC like nonsense hERG mutations.[6] A loss of function of the LTCC has been shown previously to produce the BrS phenotype.[10–13] In addition to 1 duplication and 1 deletion mutation,[4,11] previously reported *CACNA1C* variants were mostly missense mutations and all reduced reconstituted

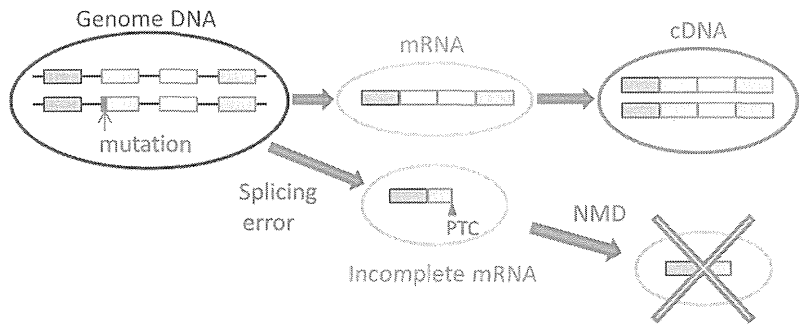

Figure 4 A model of the splicing error and nonsense-mediated mRNA decay (NMD) in the patient's messenger RNA (mRNA). The blue circle indicates genomic DNA; the yellow circle indicates mRNA; and the pink circle indicates complementary DNA (cDNA). The gray lines indicate introns, and the colored squares (blue, green, yellow, and pink) indicate exons. PTC = premature termination codon.

calcium current (I_{Ca}). In contrast, *CACNA1C*-R632R decreases I_{Ca} through a completely different mechanism.

Regarding differences in clinical severity between proband and his daughter, there may be 2 reasons: first, BrS phenotype appeared considerably depending on the sex[14]; second, proband's daughter is still 13 years old, and most patients with BrS became diagnosable around the age of 30 years or more; in addition, the mean age at cardiac event was 30 years.[15] Our proband had the first cardiac event at the age of 27 years. We need to carefully observe his daughter's clinical course. In addition, expression levels of mRNA might not be necessarily equal in spite of the same mutation; therefore, the difference in the mRNA expression level may also affect their severity of phenotype.

For cases with documented VF, ICD implantation is recommended (class I).[2,16] As medication, quinidine and isoproterenol are recommended. In addition, cilostazol, which is a phosphodiesterase III inhibitor, normalizes the ST segment most likely by augmenting the I_{Ca}, as well as by reducing transient outward potassium current (I_{to}) secondary to an increase in heart rate.[17] In diseases caused by NMD, such as cystic fibrosis, an aminoglycoside antibiotic treatment has been tested, which induced PTC suppression and resulted in functional improvement. If recognition of stop codons is suppressed by the drug, the NMD machinery does not recognize transcripts containing PTCs and proteins are synthesized like missense mutation.[5] A pharmacogenetic approach, however, has to await further examination.

Study limitations

Although we hypothesized that the *CACNA1C* splicing mutation would induce NMD and loss of function of the LTCC like nonsense hERG mutations, this study has a few limitations. In the minigene analysis, the expected skipping of exon 14 was not observed in our experimental setting. In addition, the sequences of the resulting cDNA products were altered in both the wild type and mutant, indicating that the splicing machinery for the minigenes in the HEK293 cells was different from that in human tissues. Therefore, our minigene experiment does not necessarily rule out the possibility of a mutation-related splicing error. In addition, quantification of Cav1.2 protein level could not be performed in this study. We considered an experiment examining different exon splicing mechanisms in vivo and in vitro; however, it would be too difficult to control for in vivo differences.

Conclusions

We showed the BrS proband carrying a splicing mutation of *CACNA1C*. The loss of function of the LTCC by this mutation can be suggestive of a decrease in mutant mRNAs induced by NMD, which subsequently alters the amount of mRNA.

Acknowledgments

We are grateful to Ms Arisa Ikeda and Ms Aya Umehara for screening of the *KCNQ1*, *KCNH2*, and *SCN5A* genes.

Appendix

Supplementary data

Supplementary data associated with this article can be found in the online version at http://dx.doi.org/10.1016/j.hrthm.2013.12.011.

References

1. Brugada P, Brugada J. Right bundle branch block, persistent ST segment elevation and sudden cardiac death: a distinct clinical and electrocardiographic syndrome. A multicenter report. J Am Coll Cardiol 1992;20:1391–1396.
2. Antzelevitch C, Brugada P, Borggrefe M, et al. Brugada syndrome: report of the second consensus conference: Endorsed by the Heart Rhythm Society and the European Heart Rhythm Association. Circulation 2005;111:659–670.
3. Kapplinger JD, Tester DJ, Alders M, et al. An international compendium of mutations in the SCN5A-encoded cardiac sodium channel in patients referred for Brugada syndrome genetic testing. Heart Rhythm 2010;7:33–46.
4. Burashnikov E, Pfeiffer R, Barajas-Martinez H, et al. Mutations in the cardiac L-type calcium channel associated with inherited J-wave syndromes and sudden cardiac death. Heart Rhythm 2010;7:1872–1882.
5. Holbrook JA, Neu-Yilik G, Hentze MW, Kulozik AE. Nonsense-mediated decay approaches the clinic. Nat Genet 2004;36:801–808.
6. Gong Q, Zhang L, Vincent GM, Horne BD, Zhou Z. Nonsense mutations in hERG cause a decrease in mutant mRNA transcripts by nonsense-mediated mRNA decay in human long-QT syndrome. Circulation 2007;116:17–24.
7. Murray A, Donger C, Fenske C, et al. Splicing mutations in KCNQ1: a mutation hot spot at codon 344 that produces in frame transcripts. Circulation 1999;100:1077–1084.
8. Tsuji K, Akao M, Ishii TM, et al. Mechanistic basis for the pathogenesis of long QT syndrome associated with a common splicing mutation in KCNQ1 gene. J Mol Cell Cardiol 2007;42:662–669.
9. Fukuyama M, Ohno S, Wang Q, et al. L-type calcium channel mutations in Japanese patients with inherited arrhythmias. Circ J 2013;77:1799–1806.
10. Antzelevitch C, Pollevick GD, Cordeiro JM, et al. Loss-of-function mutations in the cardiac calcium channel underlie a new clinical entity characterized by ST-segment elevation, short QT intervals, and sudden cardiac death. Circulation 2007;115:442–449.
11. Napolitano C, Antzelevitch C. Phenotypical manifestations of mutations in the genes encoding subunits of the cardiac voltage-dependent L-type calcium channel. Circ Res 2011;108:607–618.
12. Kanter RJ, Pfeiffer R, Hu D, Barajas-Martinez H, Carboni MP, Antzelevitch C. Brugada-like syndrome in infancy presenting with rapid ventricular tachycardia and intraventricular conduction delay. Circulation 2012;125:14–22.
13. Venetucci L, Denegri M, Napolitano C, Priori SG. Inherited calcium channelopathies in the pathophysiology of arrhythmias. Nat Rev Cardiol 2012;9:561–575.
14. Hong K, Berruezo-Sanchez A, Poungvarin N, et al. Phenotypic characterization of a large European family with Brugada syndrome displaying a sudden unexpected death syndrome mutation in SCN5A. J Cardiovasc Electrophysiol 2004;15:64–69.
15. Priori SG, Napolitano C, Gasparini M, et al. Natural history of Brugada syndrome: insights for risk stratification and management. Circulation 2002;105:1342–1347.
16. Priori SG, Wilde AA, Horie M, et al. HRS/EHRA/APHRS Expert Consensus Statement on the Diagnosis and Management of Patients with Inherited Primary Arrhythmia Syndromes: Document endorsed by HRS, EHRA, and APHRS in May 2013 and by ACCF, AHA, PACES, and AEPC in June 2013. Heart Rhythm 2013;10:1932–1963.
17. Tsuchiya T, Ashikaga K, Honda T, Arita M. Prevention of ventricular fibrillation by cilostazol, an oral phosphodiesterase inhibitor, in a patient with Brugada syndrome. J Cardiovasc Electrophysiol 2002;13:698–701.

Original Article

Novel Calmodulin Mutations Associated With Congenital Arrhythmia Susceptibility

Naomasa Makita, MD, PhD*; Nobue Yagihara, MD*; Lia Crotti, MD, PhD*; Christopher N. Johnson, PhD*; Britt-Maria Beckmann, MD; Michelle S. Roh; Daichi Shigemizu, PhD; Peter Lichtner, PhD; Taisuke Ishikawa, DVM, PhD; Takeshi Aiba, MD, PhD; Tessa Homfray, MBBS; Elijah R. Behr, MBBS, MD; Didier Klug, MD; Isabelle Denjoy, MD; Elisa Mastantuono, MD; Daniel Theisen, MD; Tatsuhiko Tsunoda, PhD; Wataru Satake, MD, PhD; Tatsushi Toda, MD, PhD; Hidewaki Nakagawa, MD, PhD; Yukiomi Tsuji, MD, PhD; Takeshi Tsuchiya, MD; Hirokazu Yamamoto, MD; Yoshihiro Miyamoto, MD, PhD; Naoto Endo, MD, PhD; Akinori Kimura, MD, PhD; Kouichi Ozaki, PhD; Hideki Motomura, MD; Kenji Suda, MD, PhD; Toshihiro Tanaka, MD, PhD; Peter J. Schwartz, MD; Thomas Meitinger, MD; Stefan Kääb, MD, PhD; Pascale Guicheney, PhD; Wataru Shimizu, MD, PhD; Zahurul A. Bhuiyan, MD, PhD; Hiroshi Watanabe, MD, PhD; Walter J. Chazin, PhD; Alfred L. George, Jr, MD

Background—Genetic predisposition to life-threatening cardiac arrhythmias such as congenital long-QT syndrome (LQTS) and catecholaminergic polymorphic ventricular tachycardia (CPVT) represent treatable causes of sudden cardiac death in young adults and children. Recently, mutations in calmodulin (*CALM1*, *CALM2*) have been associated with severe forms of LQTS and CPVT, with life-threatening arrhythmias occurring very early in life. Additional mutation-positive cases are needed to discern genotype–phenotype correlations associated with calmodulin mutations.

Methods and Results—We used conventional and next-generation sequencing approaches, including exome analysis, in genotype-negative LQTS probands. We identified 5 novel de novo missense mutations in *CALM2* in 3 subjects with LQTS (p.N98S, p.N98I, p.D134H) and 2 subjects with clinical features of both LQTS and CPVT (p.D132E, p.Q136P). Age of onset of major symptoms (syncope or cardiac arrest) ranged from 1 to 9 years. Three of 5 probands had cardiac arrest and 1 of these subjects did not survive. The clinical severity among subjects in this series was generally less than that originally reported for *CALM1* and *CALM2* associated with recurrent cardiac arrest during infancy. Four of 5 probands responded to β-blocker therapy, whereas 1 subject with mutation p.Q136P died suddenly during exertion despite this treatment. Mutations affect conserved residues located within Ca^{2+}-binding loops III (p.N98S, p.N98I) or IV (p.D132E, p.D134H, p.Q136P) and caused reduced Ca^{2+}-binding affinity.

Conclusions—*CALM2* mutations can be associated with LQTS and with overlapping features of LQTS and CPVT. ***(Circ Cardiovasc Genet.* 2014;7:466-474.)**

Key Words: calmodulin ■ long QT syndrome

Congenital long-QT syndrome (LQTS) is a recognizable and treatable genetic predisposition to sudden cardiac death in children and young adults.[1] Considerable genetic heterogeneity underlies this syndrome, although a large fraction of successfully genotyped LQTS subjects belong to 3 major subtypes (LQT1, LQT2, and LQT3) associated with mutations in 3 genes encoding plasma membrane ion channels (*KCNQ1*, *KCNH2*, and *SCN5A*, respectively). Distinct genotype-specific patterns of T-wave morphology,[2,3] triggers for cardiac events,[4] clinical outcomes,[5] and response to the epinephrine provocation test[6,7] have been observed. Importantly, genotype can also influence the response to specific drug therapy.[8–11] Genetic testing for known arrhythmia susceptibility genes has become standard of care for some disorders including LQTS, but despite the rapid progress in understanding the genetic basis, the cause remains unknown in many cases.[12] Additional studies are needed to reveal the

Clinical Perspective on p 474

Received November 27, 2013; accepted May 8, 2014.

*Drs Makita, Yagihara, Crotti, and Johnson contributed equally to this work.

The Data Supplement is available at http://circgenetics.ahajournals.org/lookup/suppl/doi:10.1161/CIRCGENETICS.113.000459/-/DC1.

Correspondence to Naomasa Makita, MD, PhD, Department of Molecular Physiology, Nagasaki University Graduate School of Biomedical Sciences, 1-12-4 Sakamoto, Nagasaki, 852-8523, Japan. E-mail makitan@nagasaki-u.ac.jp or Alfred L. George, Jr, MD, Department of Pharmacology, Northwestern University, Feinberg School of Medicine, 320 E Superior St, Chicago, IL 60611. E-mail al.george@northwestern.edu

Circ Cardiovasc Genet **is available at http://circgenetics.ahajournals.org** **DOI: 10.1161/CIRCGENETICS.113.000459**

missing heritable factors and to elucidate genotype–phenotype correlations.

Recently, mutations in 2 of 3 genes encoding identical peptide sequences for the essential Ca^{2+}-signaling protein calmodulin were associated with life-threatening arrhythmia predisposition, including malignant forms of LQTS, catecholaminergic polymorphic ventricular tachycardia (CPVT), and idiopathic ventricular tachycardia.[13–15] Nyegaard et al[13] identified 2 distinct missense *CALM1* (p.N54I, p.N98S) mutations in association with CPVT. Crotti et al[14] used exome sequencing and targeted resequencing to discover novel *CALM1* (p.D130G, p.F142L) and *CALM2* (p.D96V) missense mutations in subjects with infantile or perinatal presentations of severe LQTS associated with recurrent cardiac arrest. Most recently, Marsman et al[15] identified a novel *CALM1* mutation (F90L) segregating with idiopathic ventricular tachycardia and sudden death in a Moroccan family. Although this limited number of calmodulin mutations suggests preliminary genotype–phenotype correlations, additional mutations are needed to establish the spectrum of clinical features and severity of arrhythmia phenotypes associated with calmodulin mutations.

Here we report the discovery of 5 novel de novo missense *CALM2* mutations associated with congenital arrhythmia susceptibility in probands of varying ancestry. The mutations alter conserved residues that directly coordinate Ca^{2+} ions in the carboxyl-terminal domain of calmodulin and cause significant reductions in Ca^{2+}-binding affinity. Clinical and electrophysiological findings in these subjects suggested that *CALM2* mutations can be associated with less severe forms of LQTS compared with our previous report[14] as well as with overlapping clinical features of LQTS and CPVT.

Methods

Study Subjects

The QT interval was corrected for heart rate using Bazett formula ($QTc=QT/\sqrt{RR}$), and the diagnosis of LQTS was made by the Schwartz criteria.[1] All individuals who participated in the study gave written informed consent before genetic and clinical investigations in accordance with the standards of the Declaration of Helsinki and the local ethics committees at each participating institution. We studied 2 Japanese cohorts, 1 consisting of 12 unrelated LQTS subjects who were without a genetic diagnosis after sequencing genes previously associated with life-threatening arrhythmias (*KCNQ1*, *KCNH2*, *SCN5A*, *SCN1B*, *SCN2B*, *SCN3B*, *SCN4B*, *KCNE1*, *KCNE2*, *KCNJ2*, and *CAV3*)[13,14,16] and another cohort consisting of 190 unrelated patients with LQTS in whom whole exome sequencing was performed. Exome sequencing was performed on a parent/child trio in which the proband was a child who suffered cardiac arrest at age of 17 months. A German mutation-negative LQTS proband and a Moroccan girl with sudden cardiac death were also screened for mutations in *CALM1*, *CALM2*, and *CALM3*.

Candidate Gene and Exome Sequencing

Targeted exon capture was performed for 240 candidate arrhythmia susceptibility genes (Table I in the Data Supplement) using the SureSelect Target Enrichment System according to the manufacturer's suggestions (Agilent Technologies, Inc., Santa Clara, CA). The captured DNA was sequenced on the Genome Analyzer IIx platform (Illumina Inc., San Diego, CA) with paired-end reads of 101 bp for insert libraries consisting of 150 to 200 bp fragments. On average for targeted capture sequencing, 1.1 Gbp of short-read sequence data were generated and 98.9% were mapped to the reference human genome. Whole exome capture was performed using Agilent SureSelect Human All Exon V4 reagent, and captured DNA was sequenced on Illumina HiSeq2000 (performed at RIKEN) or HiSeq2500 (performed at Vanderbilt University) platforms. For data obtained on the HiSeq2000, an average of 6.4 Gbp of short-read sequence data were generated, with 98.6% mapped successfully to the reference human genome and 66-fold average coverage for all captured exons. For data obtained on the HiSeq2500, an average of 5.8 Gbp was generated per subject with 99.8% mapped and 50-fold average coverage.

Sequence Data Analysis

Sequence reads were mapped to the human reference genome (GRCh37) using the Burrows-Wheeler Aligner (version 0.6.1).[17] Possible duplicate reads were removed using SAMtools[18] and custom software, leaving an average of 0.8 and 5.5 Gb for targeted capture and exome sequencing, respectively. More than 93% of targeted regions were covered by ≤10 reads. After filtering by pair mapping distance, mapping uniqueness, and orientation between paired reads, the mapping result files were converted into the pileup format using SAMtools.[18] Variant calling was conducted in part on the basis of published methods.[19–21] We further used the following quality control filters: (1) alignments near putative indels were refined using GATK,[22] and (2) a strand bias filter excluded variants whose alternative allele was preferentially found on 1 of the 2 available read orientations at the site. Variants found in dbSNP Build 137, 1000 Genomes,[23] or Exome Variant Server (EVS)[24] databases were excluded from further analyses. Synonymous and intronic (other than canonical splice sites) variants were also excluded. Three other exome databases (RIKEN database of 731 noncardiac disease Japanese exomes, Human Genetic Variation Browser database including exome data obtained from 1208 Japanese subjects [http://www.genome.med.kyoto-u.ac.jp/SnpDB], and the Institute of Human Genetics Helmholtz Zentrum München database of >3000 exomes of European ancestry) were also queried for candidate mutations.

Additional Mutation Detection

Targeted PCR–Sanger sequencing was performed as described previously[14] on DNA from a German woman with clinical features of LQTS and CPVT, as well as in a Moroccan girl with sudden cardiac death and a presumptive diagnosis of CPVT to search for variants in the coding exons of *CALM1*, *CALM2*, and *CALM3*. Variants discovered by exome sequencing were also confirmed by Sanger sequencing using an automated capillary electrophoresis DNA sequencing platform (Applied Biosystems, Foster City, CA), then further annotated based on evolutionary amino acid conservation (Mutation Taster),[25] and predicted impact on protein function (Polyphen2, SIFT).[26,27] Mutation position in calmodulin was based on RefSeq NP_001734 counting the predicted translational start codon (Met) as position 1.

Expression of Recombinant Calmodulins and Measurement of Ca^{2+} Affinity

Biochemical studies of recombinant calmodulin proteins were performed as previously described.[14] Briefly, recombinant wild-type and mutant calmodulins were expressed in *Escherichia coli* and purified by standard chromatographic approaches. Macroscopic affinity constants for Ca^{2+} binding in the amino-terminal and carboxy-terminal domains were determined by measuring changes in intrinsic fluorescence as reported by Shea et al.[28,29] The data were analyzed by plotting the normalized fluorescence signal versus free Ca^{2+} concentration and fitting to a 2-site Adair function for each domain.[30,31]

Results

Case Presentations

Case 1

A 6-year-old Japanese girl was admitted to the hospital for evaluation of syncope and a markedly prolonged QT interval. She had a history of fetal bradycardia but had an uneventful birth. She had her first episode of syncope at the age of 19

months. An ECG at that time showed marked QT prolongation (QTc=579 ms) with atypical notched, late-peaking T waves (Figure 1A). Atrial pacing at 100 bpm prolonged QTc from 596 to 619 ms, whereas mexiletine shortened QTc from 596 to 550 ms (Figure 1B). Subsequently, she experienced multiple episodes of cardiac arrest during exertion when she failed to take mexiletine, prompting placement of an implantable cardioverter defibrillator (ICD) at the age of 14 years. Medical therapy with mexiletine and a β-adrenergic receptor blocker atenolol was generally effective in preventing ventricular arrhythmias, although there was an episode of appropriate ICD discharge that occurred during exertion. The patient had no history of seizures or developmental delay. Genetic testing for mutations in *KCNQ1*, *KCNH2*, *SCN5A*, *SCN1B*, *SCN2B*, *SCN3B*, *SCN4B*, *KCNE1*, *KCNE2*, *KCNJ2*, and *CAV3* was negative. There was no family history of LQTS or sudden death, and both parents had normal QTc intervals (father 369 ms, mother 394 ms) as did her 2 brothers (368, 388 ms).

Case 2

A 5-year-old Japanese boy had an episode of syncope with seizure while running. Two months later, he had a similar episode and was evaluated in an emergency room. An ECG exhibited QTc prolongation (478 ms; Figure 2A), whereas echocardiogram, electroencephalogram, and brain MRI were normal. He showed no developmental delay. There was no family history of arrhythmias or sudden death, and both parents (father 364 ms, mother 396 ms) and his brother (340 ms) had normal QTc intervals. Epinephrine infusion test did not induce ectopic beats but caused marked QTc prolongation (baseline heart rate/QT/QTc, 56 bpm/484 ms/466 ms; peak heart rate/QT/QTc, 94 bpm/446 ms/558 ms; steady-state heart rate/QT/QTc, 73 bpm/484 ms/535 ms; Figure 2B). This subject did not tolerate exercise testing because of dizziness. Genetic testing for mutations in *KCNQ1*, *KCNH2*, *SCN5A*, *KCNE1*, *KCNE2*, *KCNJ2*, and *AKAP9* was negative. Treatment with propranolol alone or in combination with mexiletine shortened the QTc interval to 471 to 473 ms (Figure 2C), but he continued to experience syncope and dizziness while running. The drugs were replaced with metoprolol at the age of 11 years. Subsequently, he had no further episodes of syncope, and there was normalization of the QTc (449 ms) with elimination of the notch in the descending limb of the T wave (Figure 2C).

Case 3

A 29-year-old German woman, who was previously diagnosed with perinatal bradycardia and neonatal LQTS, had been treated with pindolol. Her family history was negative for cardiac arrest and sudden death. On β-blocker therapy, she remained asymptomatic until the age of 9 years when she suffered syncope while swimming after an interruption of therapy. At that time, there was evidence of exercise-induced polymorphic ventricular ectopy. She became asymptomatic for several years after resumption of treatment with various β-blockers (pindolol, propranolol, atenolol). Her resting ECG exhibited QT prolongation (465–578 ms) with persistent biphasic T waves in leads III, aVF, aVL, V3, and negative T waves in V4 to V6 (Figure 3A). The patient never suffered seizures, and she had normal physical and mental development. At the age of 22 years, exercise-induced polymorphic ventricular ectopy and one 3-beat run of polymorphic ventricular tachycardia was documented (Figure 3B; Figure I in the Data Supplement). Echocardiographic evaluation was normal, but MRI revealed features consistent with noncompaction of the left ventricle myocardium. Both parents had normal QTc intervals (father 407 ms, mother 377 ms) with no signs of polymorphic ventricular arrhythmias. Directed screening of genes involved with LQTS and CPVT (*KCNQ1*, *KCNH2*, *SCN5A*, *KCNE1*, *KCNE2*, *KCNJ2*, *ANK2*, *CAV3*, *KCNE3*, *SNTA1*, *RYR2*, *CASQ2*) was negative for mutations.

Case 4

A Moroccan girl from a family with no history of cardiac arrhythmia was hospitalized at the age of 8 years after an episode of syncope associated with prolonged period of unconsciousness. At that time, she had a prolonged QTc interval (500 ms) with ventricular bigeminy. A Holter recording demonstrated prolonged QTc interval (ECG images were not available). Echocardiographic evaluation was normal. Both parents and 4 female siblings were asymptomatic. The subject was

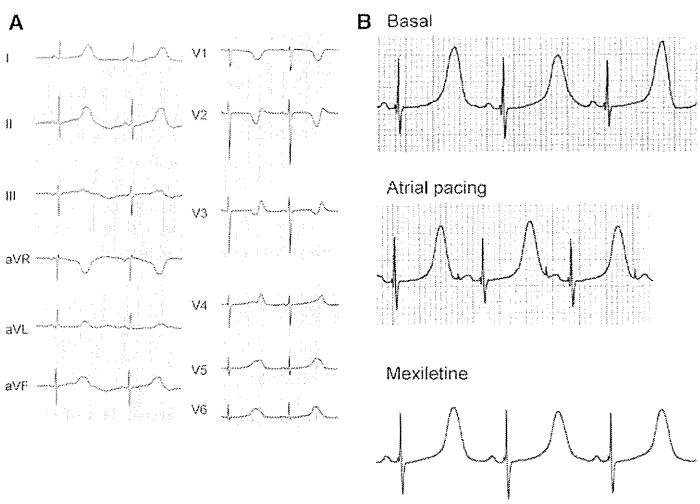

Figure 1. Electrocardiographic abnormalities in case 1. **A**, Standard 12-lead ECG recorded at age 6 y showing marked QTc prolongation (579 ms) with atypical T-wave morphology (late-peaking with notch on the descending limb). **B**, Atrial pacing at 100 bpm prolonged QTc from 596 to 610 ms. By contrast, mexiletine treatment shortened QT interval from 596 to 550 ms.

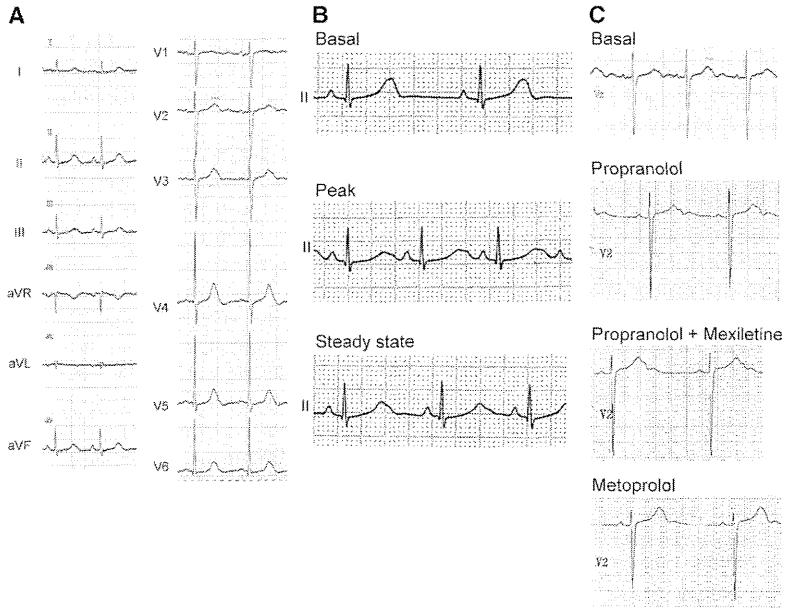

Figure 2. Electrocardiographic abnormalities in case 2. **A**, Standard 12-lead ECG recorded at age 5 y showing QTc prolongation (478 ms). **B**, Epinephrine challenge test prolonged QTc at peak (466 to 558 ms) and at steady state (535 ms). **C**, Propranolol or propranolol with mexieltine caused QTc shortening from 517 to 471 and 473 ms, respectively. Metoprolol normalized QTc to 449 ms.

treated with nadolol (40 mg per day) and she remained asymptomatic with QTc intervals ranging from 420 to 450 ms without ventricular ectopy. Unfortunately, she died suddenly at the age of 11 years while dancing at a wedding in Morocco. The initial diagnosis was LQTS, and later a diagnosis of CPVT was considered because of clinical circumstances and ventricular ectopy. No exercise stress test was performed. No neurological dysfunction was reported and a head computed tomographic scan was normal. Genetic testing was negative for *KCNQ1*, *KCNH2*, *SCN5A*, *KCNE1*, *RYR2*, *CASQ2*, and *TRDN*.

Case 5

A previously healthy white boy from England suffered cardiac arrest secondary to ventricular fibrillation at the age of 17 months, and he was promptly resuscitated. ECG showed bradycardia and a prolonged QTc interval (555 ms; Figure 4). There was no family history of cardiac arrhythmia, and both parents were healthy with normal QTc interval duration. There were no siblings. An ICD was placed soon after the cardiac arrest, and no discharges were documented over the ensuing 13 months. The subject was also treated with β-blockers. Genetic testing for mutations *KCNQ1*, *KCNH2*, *SCN5A*, *KCNE1*, and *KCNE2* was negative.

A summary of clinical features observed in the 5 cases is presented in Table.

Discovery of Novel *CALM2* Mutations

To identify mutations in candidate arrhythmia susceptibility genes, a custom targeted exon capture probe panel

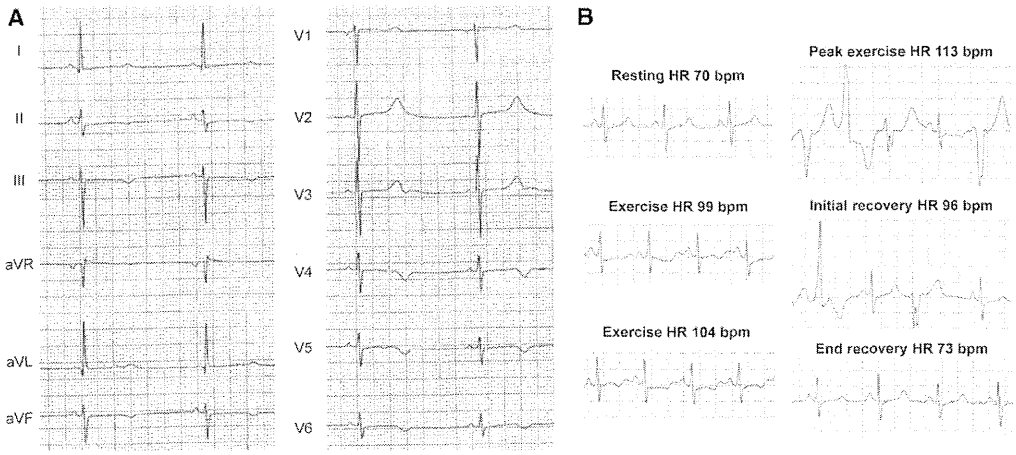

Figure 3. Electrocardiographic features of case 3. **A**, Standard 12-lead ECG recorded at age 27 y showing QTc prolongation (567 ms). **B**, Polymorphic ventricular ectopy recorded (lead III) during exercise (step test) at age 28 y. During exercise, a progressive increase of heart rate was observed with no arrhythmias until 110 bpm was reached. A 3-beat episode of polymorphic ventricular tachycardia was recorded at 113 bpm. A representative 12-lead ECG during exercise is provided as Figure I in the Data Supplement.

interrogating 240 genes (Table I in the Data Supplement) was used to screen 12 unrelated mutation-negative Japanese LQTS probands using a next-generation sequencing platform resulting in an average 187-fold coverage of targeted regions (additional details of the method will be reported elsewhere). A heterozygous nonsynonymous single-nucleotide variant (c.400G>C; Figure 5A) in exon 5 of *CALM2* was identified in a 6-year-old girl (described above as case 1). The nucleotide change predicts the substitution of a conserved aspartic acid residue with histidine (p.D134H) within the fourth EF-hand Ca^{2+}-binding motif in the C-terminal domain of the encoded calmodulin protein. The location of this variant within the protein was 4 residues away from a mutation (p.D130G) previously associated with a very severe form of infantile LQTS (Figure 5B and 5C).[14] This variant was not found in her parents nor her 2 brothers and is absent in dbSNP, 1000 Genomes, EVS, RIKEN, and Human Genetic Variation Browser exome databases consistent with a novel de novo mutation.

Motivated by this finding, we searched for other calmodulin gene (*CALM1*, *CALM2*, *CALM3*) mutations in exome sequence data (coverage was 35X, 92X, and 59X for the 3 calmodulin genes, respectively) obtained from 190 unrelated mutation-negative Japanese LQTS probands. A second heterozygous nonsynonymous variant (c.293A>G; Figure 5A) was found in *CALM2* exon 5 in a 5-year-old boy (described above as case 2) diagnosed with LQTS. This variant is predicted to replace a conserved asparagine at position 98 with serine (p.N98S) within the third EF-hand Ca^{2+}-binding motif in calmodulin (Figure 5B and 5C). Interestingly, de novo p.N98S mutation in a different calmodulin gene (*CALM1*) was previously associated with CPVT in an Iraqi female child without QT prolongation.[13] This variant was not found in her parents or brother and was absent in exome data of the other 189 LQTS probands as well as in databases of genetic variation (dbSNP, 1000 Genomes, EVS, RIKEN, and Human Genetic Variation Browser exome databases) consistent with a de novo missense mutation. The probability that 2 private nonsynonymous mutations occurred in *CALM2* among 190 Japanese samples by chance was estimated as 0.0258 (see the Data Supplement).

Exome sequencing was also performed on a 17-month-old English boy who suffered cardiac arrest in the context of LQTS (case 5) and his healthy parents (coverage averaged 30X for the 3 calmodulin genes). After excluding all variants shared with at least 1 parent, synonymous variants and common variants, the proband was found to have de novo nonsynonymous variants in 4 protein-coding genes (*CALM2*, *OBSCN*, *DLG1*, *GOLGA3*). However, only the variant identified in *CALM2* (c.A293>T; Figure 5A) predicting substitution of asparagine at position 98 in calmodulin with isoleucine (p.N98I; Figure 5B and 5C) was predicted to be deleterious by SIFT and probably damaging by PolyPhen-2. This variant occurs at the same position as the *CALM2* mutation discovered in case 2 (LQTS) and a previously reported *CALM1* mutation (N98S) found in a child with CPVT.[13] *CALM2*-p.N98I was absent in the previously mentioned databases.

By candidate gene screening of *CALM1*, *CALM2*, and *CALM3*, we identified 2 other heterozygous missense *CALM2* variants. One variant was discovered in a 29-year-old German woman who was diagnosed initially with neonatal LQTS and later exhibited exercise-induced polymorphic ventricular ectopy (case 3). The variant (c.396T>G; Figure 5A) predicted the replacement of a conserved aspartic acid residue at position 132 with glutamate (p.D132E) within the fourth EF-hand Ca^{2+}-binding motif in calmodulin (Figure 5B and 5C). The location of the variant is 2 amino acids N-terminal of p.D134H (case 1) and 2 residues C-terminal of the previously identified p.D130G.[14] This variant was predicted to be damaging by SIFT and Mutation Taster, whereas it was predicted to be benign by Polyphen2. The mutation was not found in the aforementioned databases of genetic variants (dbSNP, 1000 Genomes, EVS) and was also absent in the Helmholtz exome database in which mean coverage of *CALM2* was greater than 95-fold.[14] The variant was not found in her parents and, therefore, D132E was considered a likely novel de novo missense *CALM2* mutation.

The second *CALM2* variant discovered by targeted sequencing was found in an 8-year-old Moroccan girl (case 4) with presumptive diagnoses of LQTS and CPVT who died suddenly during exertion despite ongoing treatment with β-blockers. The variant (c.A407>C; Figure 5A) predicted the replacement of glutamine at position 136 with proline (p.Q136P) in the fourth EF-hand Ca^{2+}-binding motif (Figure 5B and 5C). The mutation was not found in the aforementioned databases of genetic variants (dbSNP, 1000 Genomes, EVS) and was absent in the parents and 4 siblings consistent with a de novo mutation.

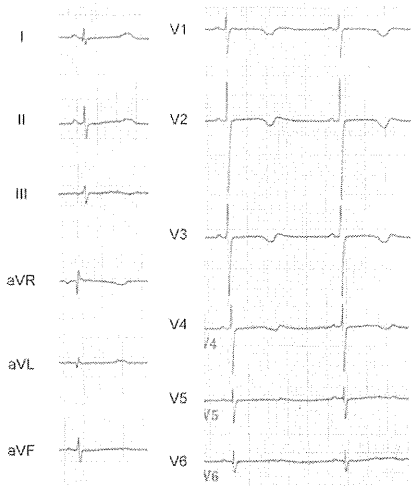

Figure 4. Electrocardiographic features of case 5. Standard 12-lead ECG recorded at age 2 y showing QTc prolongation (555 ms) and bradycardia (heart rate [HR]=55 bpm) during β-blocker treatment. Because of bradycardia, only 1 beat was recorded in the limb leads.

CALM2 Mutations Confer Impaired Ca^{2+} Affinity

We previously demonstrated that calmodulin mutations associated with early-onset LQTS confer reduced affinity for Ca^{2+}.[14] Similarly, Nyegaard et al[13] examined Ca^{2+} affinity for *CALM1* p.N98S, which they observed in a de novo case of CPVT and found a slight depression in C-domain Ca^{2+}-binding affinity. To determine the biochemical consequences

Table. Summary of Clinical Characteristics and the *CALM2* Mutations of the Probands

Subject	Sex	Age at Diagnosis (Current Age)	CA	QTc, ms	Treatment	Mutation
Case 1	F	1 y (16 y)	Yes	579	MEX, BB, ICD	*CALM2*-p.D134H
Case 2	M	5 y (12 y)	No	478	MEX, BB	*CALM2*-p.N98S
Case 3	F	Perinatal (29 y)	No	578	BB	*CALM2*-p.D132E
Case 4	F	8 y (died at age 11 y)	SCD	500	BB	*CALM2*-p.Q136P
Case 5	M	17 mo (30 mo)	Yes	555	BB, ICD	*CALM2*-p.N98I

BB indicates β-blocker; Abbreviations: CA, cardiac arrest; F, female; ICD, implantable cardioverter defibrillator; M, male; MEX, mexiletine; PVC, premature ventricular contractions; PVT, polymorphic ventricular tachycardia; and SCD, sudden cardiac death.

of the 4 novel *CALM2* mutations we identified, recombinant calmodulin proteins were generated and purified, and in vitro Ca^{2+} binding affinities were measured. None of the 4 mutations significantly affected Ca^{2+} affinity in the N-domain, but substantial effects on affinity in the C-domain were observed (Figure 6). Dissociation constants for Ca^{2+} (K_d) of 2.1±0.1, 15±1, 48±10, 27±5, and 19±2 μmol/L were determined for wild-type, N98I, D132E, D134H, and Q136P, respectively, corresponding to a 7- to 23-fold reduction in Ca^{2+}-binding affinity to the C-domain. These data demonstrate a significant functional impairment caused by the novel calmodulin variants consistent with disease-causing mutations that will likely disrupt the ability to transduce intracellular Ca^{2+} signals leading to cardiac arrhythmia susceptibility.

Discussion

The identification of new arrhythmia susceptibility genes and mutations will facilitate the prevention of sudden cardiac death through the rapid identification of at-risk populations and may illuminate new molecular targets for therapy. Here we expand the spectrum of mutations in calmodulin, a recently demonstrated cause of life-threatening heart rhythm disorders.

Calmodulin functions as a Ca^{2+} sensor in a wide range of intracellular Ca^{2+}-signaling pathways. The protein sequence is completely conserved among all vertebrates, and in humans, 3 unique genes (*CALM1*, *CALM2*, *CALM3*) encode for identical calmodulin protein.[32] In the recent reports of human calmodulin gene mutations, there was only 1 *CALM2* allele identified compared with 5 *CALM1* mutations.[13–15] The previously identified calmodulin mutations associated with LQTS phenotypes along with those we report here affect conserved residues within the 2 EF-hand motifs of the C-domain and cause substantially impaired Ca^{2+} affinity. The mutations with the greatest impact on Ca^{2+} affinity involve substitutions of conserved aspartic acid residues (D130G, D132E, D134H) known to be directly involved in coordinating Ca^{2+} ions in Ca^{2+}-binding

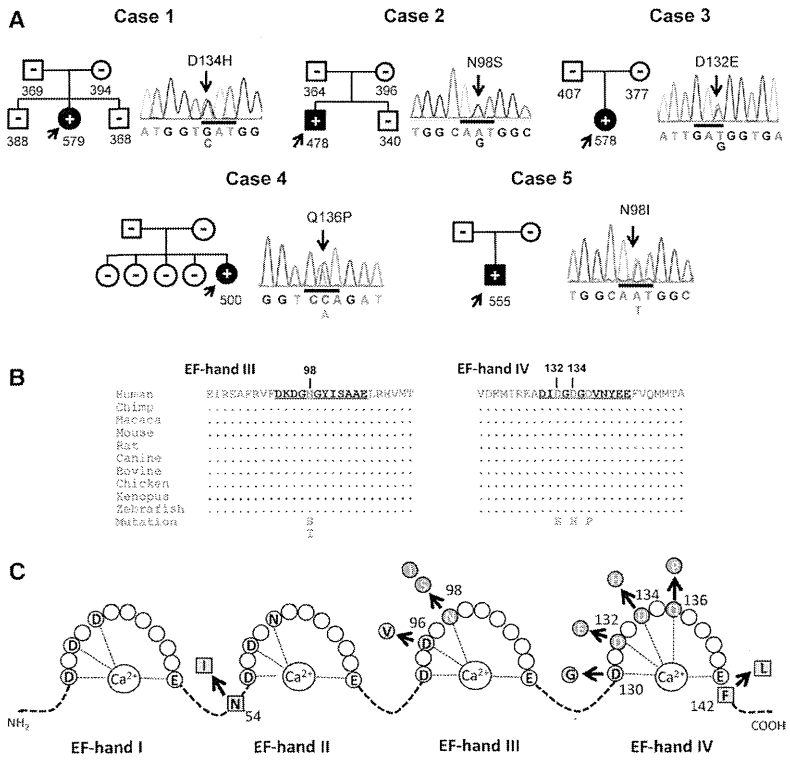

Figure 5. Novel de novo *CALM2* mutations. **A**, Pedigrees and Sanger sequence electropherograms of each proband (marked by arrow). QTc values for each individual are shown underneath the corresponding pedigree symbol. **B**, Amino acid sequence alignments for calmodulins from different species with location of the 5 missense mutations. Amino acid sequence of EF-hands III and IV are underlined. **C**, Schematic model of Ca^{2+} binding loops in the N-terminal (I and II) and C-terminal (III and IV) domains of calmodulin showing the locations of mutations. Red circles represent the *CALM2* mutations (p.N98S, p.N98I, p.D132E, p.D134H, p.Q136P) identified in our present study; green symbols represent previously reported mutations.

loop IV.[33,34] Notably, even substitution with the highly similar glutamic acid side chain in D132E has an influence on Ca^{2+} affinity. Similar effects of this subtle Asp to Glu mutation on the Ca^{2+} affinity of calmodulin have been reported.[35] Although a functional effect was not predicted in silico by PolyPhen2, it is well established that each residue in the Ca^{2+}- binding loops of calmodulin and other EF-hand proteins contribute to the biochemical functions of the protein.[36]

The cellular mechanisms responsible for arrhythmia susceptibility in the setting of calmodulin mutations are likely to be complex given the multitude of molecular interactions possible for this critically important signaling molecule. As previously speculated for LQTS,[14] dysfunctional calmodulin may disrupt Ca^{2+}-dependent inactivation of L-type Ca^{2+} channels leading to increased depolarizing current during the plateau phase of the cardiac action potential. Impaired regulation of voltage-gated sodium channels may also be evoked by certain LQTS-associated calmodulin mutations. For calmodulin mutations associated with CPVT, aberrant regulation of the sarcoplasmic reticulum ryanodine receptor/Ca^{2+} release channel (*RYR2*) is a plausible mechanism based on previous studies.[37] Interestingly, the CPVT mutations do not impair Ca^{2+} affinity to the same extent as those associated with LQTS.[13] The molecular and cellular pathophysiology of arrhythmia susceptibility in the setting of calmodulin mutations is currently under intense investigation.[38–40]

Our findings further expand the phenotypic spectrum of cardiac arrhythmias associated with calmodulin mutations. Three of the probands (cases 1, 2, 5) had a later onset of LQTS compared with what was described in the study by Crotti et al,[14] in which calmodulin mutation-positive subjects had highly malignant ventricular arrhythmias beginning very early in life. Furthermore, none of the *CALM2* mutation-positive subjects we report here had significant neurological findings, other than syncope-associated seizures (case 1), in contrast to the original report in which most subjects had seizures or developmental delays. The previously observed neurological impairments were speculated to be the result of brain injury secondary to hypoxia in the setting of recurrent cardiac arrest. The minimal or absent neurological symptoms in the probands we describe here may reflect fewer episodes of cardiac arrest or more rapid resuscitation. These new observations further imply that neurological symptoms may not be an intrinsic manifestation of calmodulin mutations.

Genotype–phenotype correlations among the calmodulin mutation-positive subjects we described may provide clues to the pathophysiological mechanisms. In particular, *CALM2*-p.D132E was identified in an adult with a history of neonatal LQTS who later developed exercise-induced polymorphic ventricular arrhythmia consistent with CPVT. Similarly, *CALM2*-p.Q136P was identified in a child with LQTS and ventricular ectopy somewhat suggestive of CPVT. We speculate that the combined clinical features of LQTS and CPVT reflect the impact of p.D132E and possibly p.Q136P on 2 principal molecular targets. Abnormal calmodulin regulation of L-type Ca^{2+} channels would account for impaired myocardial repolarization similar to Timothy syndrome,[41] whereas dysregulation of *RYR2* would lead to altered regulation of intracellular Ca^{2+} homeostasis as expected in CPVT.[42,43]

Our study also revealed that an identical amino acid substitution in 2 distinct calmodulin genes can present with different clinical phenotypes. Whereas *CALM1*-p.N98S was originally found in an Iraqi female with CPVT,[13] we identified *CALM2*-p.N98S in a Japanese male with an unambiguous LQTS phenotype (case 2). The physiological basis for this genotype–phenotype disparity is unknown, but may involve differences in the corresponding proteomes of different probands because of sex or ethnicity, or differences in regional or cell type–specific expression of *CALM1* and *CALM2*.

Except during periods of medication noncompliance, all *CALM2* mutation-positive probands described in this report were responsive to β-blockers administered alone or in combination with mexiletine. However, because of recurrent cardiac arrests during treatment lapses, cases 1 and 5 had implantation of an ICD. In our prior report of calmodulin mutations in severe LQTS, probands with de novo *CALM1* or *CALM2* mutations experienced arrhythmia recurrence on pharmacological therapy and were eventually treated with ICD implantation to reduce the risk for sudden cardiac death.[14] Similarly, symptomatic mutation-positive subjects with idiopathic ventricular tachycardia reported by Marsman et al[15] had ICD implantation. By contrast, the Swedish family segregating CPVT with mutation *CALM1*-N54I described by Nyegaard et al[13] exhibited variable responses to β-blockers alone, and only 1 of 10 living mutation-positive subjects received an ICD. None of the cases we report here underwent left cardiac sympathetic denervation.

In conclusion, we report discovery of 5 novel de novo *CALM2* mutations in association with LQTS and exertion-induced arrhythmias. The encoded mutant calmodulin proteins have impaired C-domain Ca^{2+}-binding affinity that will presumably cause dysfunction in Ca^{2+} signaling with resulting

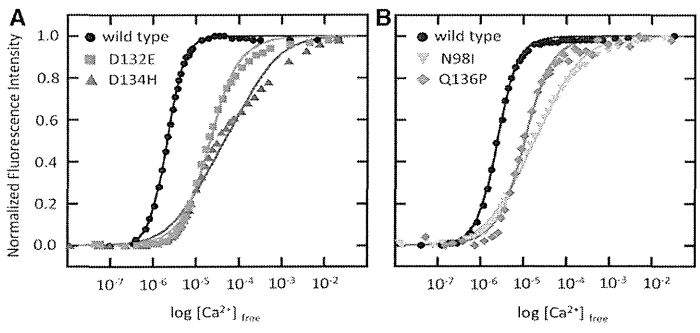

Figure 6. Impaired Ca^{2+} binding by mutant calmodulin C-domains. **A**, Representative Ca^{2+} titrations monitored by intrinsic fluorescence for recombinant wild-type (WT; black circles) and mutant calmodulins (D132E, blue triangles; D134H, red squares). K_d values derived by fitting data from 3 replicates to a 2-site model were (mean±SEM) 2.1±0.1, 48±10, and 27±5 μmol/L for WT, D132E, and D134H, respectively. **B**, Representative Ca^{2+} titrations for WT (black circles) and mutant (N98I, inverted orange triangles; Q136P, green diamonds) calmodulins. K_d values derived by fitting data from 3 replicates to a 2-site model were (mean±SEM) 2.3±0.1, 19±2, and 15±1 μmol/L for WT, N98I, and Q136P, respectively.

adverse effects on plasma membrane ion channels, intracellular membrane ion channels, or possibly both. Therapy with β-blockers was successful in preventing life-threatening exertion-triggered arrhythmias. Our study provides new evidence of congenital arrhythmia susceptibility caused by calmodulin mutations, provides further information regarding genotype–phenotype correlation, and expands the allelic diversity within *CALM2*. Calmodulin gene mutations should be sought in pediatric cases of LQTS and CPVT for whom other genetic candidates have been excluded. Because of the predominance of de novo mutations, calmodulin genes could be considered especially when both parents are unaffected.

Acknowledgments

We thank Professor Tohru Minamino for helpful suggestions; Christian Shaffer for assistance with exome data analysis; and Ryo Yamaguchi, Eriko Kojima, Saori Nakano, Atsuko Iida, Caroline Jan, and Jennifer Kunic for technical assistance. *CALM2* mutation data were submitted to ClinVar (http://www.ncbi.nlm.nih.gov/clinvar/).

Sources of Funding

This work was supported by a Grant-in-Aid for Scientific Research on Innovative Areas (HD Physiology; 22136007 to Dr Makita), a Grant-in-Aid for Scientific Research B (24390199 to Dr Makita), a Grant-in-Aid for Project in Sado for Total Health (to Dr Watanabe) from the Japanese Ministry of Education, Culture, Sports, Science and Technology, the Joint Usage/Research Program of Medical Research Institute Tokyo Medical and Dental University (to Drs Makita and Kimura), Research Grant for the Cardiovascular Diseases (H24-033) from the Japanese Ministry of Health, Labour, and Welfare (to Drs Makita, Aiba, Miyamoto, Tanaka, Shimizu, and Watanabe), the Italian Ministry of Education, University and Research (FIRB RBFR12I3KA to Dr Crotti, and PRIN 2010BWY8E9 to Drs Schwartz and Crotti), the Italian Ministry of Health (GR-2010-2305717 to Dr Crotti), the Fondation Suisse de Cardiologie (number 12341 to Dr Bhuiyan), National Institutes of Health (HL083374 to Dr George and AI101171 to Dr Chazin), and fellowship support from the National Institutes of Health (T32 NS007491 to Dr Johnson) and the American Heart Association (POST 14380036 to Dr Johnson).

Disclosures

None.

Appendix

From the Departments of Molecular Physiology (N.M., T.I., Y.T.) and Pediatrics (H.Y., H.M.), Nagasaki University Graduate School of Biomedical Sciences, Nagasaki, Japan; Department of Cardiovascular Biology and Medicine (N.Y., H,W,) and Division of Orthopedic Surgery (N.E.), Niigata University Graduate School of Medical and Dental Sciences, Niigata, Japan; Section of Cardiology, Department of Molecular Medicine, University of Pavia, Pavia, Italy (L.C.); Institute of Human Genetics, Helmholtz Zentrum München, Neuherberg, Germany (L.C., P.L., E.M., T.M.); Department of Biochemistry, Center for Structural Biology (C.N.J., M.S.R., W.J.C.), and Division of Genetic Medicine, Department of Medicine (A.L.G.), Vanderbilt University, Nashville, TN; Department of Medicine I (B.-M.B., S.K.) and Institute for Clinical Radiology (D.T.), Klinikum Grosshadern, Ludwig-Maximilians University, Munich, Germany; Laboratory for Medical Science Mathematics (D.S., T. Tsunoda) and Laboratory for Cardiovascular Diseases (K.O., T. Tanaka), RIKEN Center for Integrative Medical Sciences, Yokohama, Japan; Departments of Cardiovascular Medicine (T.A., W.Shimizu) and Preventive Cardiology (Y.M.), National Cerebral and Cardiovascular Center, Suita, Japan; Department of Genetics (T.H.) and Cardiovascular Sciences Research Centre (E.R.B.), St. George's University of London, London, United Kingdom; Hôpital Cardiologique de Lille, Service de Cardiologie, Lille, France (D.K.); Inserm, UMR_S1166, Institute of Cardiometabolism and Nutrition, Paris, France (I.D., P.G.); AP-HP, Service de Cardiologie, Hôpital Bichat, and Centre de Référence sur les Maladies Cardiaques Héréditaires, Paris, France (I.D.); Department of Neurology, Kobe University Graduate School of Medicine, Kobe, Japan (W.Satake, T.Toda); Laboratory for Genome Sequencing Analysis (H.N.) and EP Expert Doctors-Team Tsuchiya (T. Tsuchiya), Kumamoto, Japan; Department of Molecular Pathogenesis, Medical Research Institute (A.K.), and Department of Human Genetics and Disease Diversity (T . Tanaka), Tokyo Medical and Dental University, Tokyo, Japan; Department of Pediatrics and Child Health, Cardiovascular Research Institute, Kurume University School of Medicine, Kurume, Japan (K.S.); IRCCS Istituto Auxologico Italiano, Center for Cardiac Arrhythmias of Genetic Origin and Laboratory of Cardiovascular Genetics, Milan, Italy (L.C., P.J.S.); Deutsches Zentrum für Herz-Kreislauf-Forschung, Munich Heart Alliance, Munich, Germany (T.M., S.K.); Institute of Human Genetics, Technische Universität München, Munich, Germany (T.M.); Sorbonne Universités, UPMC Univ Paris 06, UMR_S1166, Institut de Recherche sur les Maladies Cardiovasculaires, du Métabolisme et de la Nutrition, Paris, France (P.G.); Department of Cardiovascular Medicine, Nippon Medical School, Tokyo, Japan (W.Shimizu); and Laboratoire de Génétique Moléculaire, Service de Génétique Médicale, Centre Hospitalier Universitaire Vaudois, Lausanne, Switzerland (Z.A.B.).

References

1. Schwartz PJ, Crotti L, Insolia R. Long-QT syndrome: from genetics to management. *Circ Arrhythm Electrophysiol*. 2012;5:868–877.
2. Moss AJ, Zareba W, Benhorin J, Locati EH, Hall WJ, Robinson JL, et al. ECG T-wave patterns in genetically distinct forms of the hereditary long QT syndrome. *Circulation*. 1995;92:2929–2934.
3. Zhang L, Timothy KW, Vincent GM, Lehmann MH, Fox J, Giuli LC, et al. Spectrum of ST-T-wave patterns and repolarization parameters in congenital long-QT syndrome: ECG findings identify genotypes. *Circulation*. 2000;102:2849–2855.
4. Schwartz PJ, Priori SG, Spazzolini C, Moss AJ, Vincent GM, Napolitano C, et al. Genotype-phenotype correlation in the long-QT syndrome: gene-specific triggers for life-threatening arrhythmias. *Circulation*. 2001;103:89–95.
5. Zareba W, Moss AJ, Schwartz PJ, Vincent GM, Robinson JL, Priori SG, et al. Influence of genotype on the clinical course of the long-QT syndrome. International Long-QT Syndrome Registry Research Group. *N Engl J Med*. 1998;339:960–965.
6. Shimizu W, Noda T, Takaki H, Kurita T, Nagaya N, Satomi K, et al. Epinephrine unmasks latent mutation carriers with LQT1 form of congenital long-QT syndrome. *J Am Coll Cardiol*. 2003;41:633–642.
7. Shimizu W, Noda T, Takaki H, Nagaya N, Satomi K, Kurita T, et al. Diagnostic value of epinephrine test for genotyping LQT1, LQT2, and LQT3 forms of congenital long QT syndrome. *Heart Rhythm*. 2004;1:276–283.
8. Schwartz PJ, Priori SG, Locati EH, Napolitano C, Cantù F, Towbin JA, et al. Long QT syndrome patients with mutations of the SCN5A and HERG genes have differential responses to Na+ channel blockade and to increases in heart rate. Implications for gene-specific therapy. *Circulation*. 1995;92:3381–3386.
9. Vincent GM, Schwartz PJ, Denjoy I, Swan H, Bithell C, Spazzolini C, et al. High efficacy of beta-blockers in long-QT syndrome type 1: contribution of noncompliance and QT-prolonging drugs to the occurrence of beta-blocker treatment "failures". *Circulation*. 2009;119:215–221.
10. Shimizu W, Aiba T, Antzelevitch C. Specific therapy based on the genotype and cellular mechanism in inherited cardiac arrhythmias. Long QT syndrome and Brugada syndrome. *Curr Pharm Des*. 2005;11:1561–1572.
11. Schwartz PJ, Ackerman MJ. The long QT syndrome: a transatlantic clinical approach to diagnosis and therapy. *Eur Heart J*. 2013;34:3109–3116.
12. Schwartz PJ, Ackerman MJ, George AL Jr, Wilde AA. Impact of genetics on the clinical management of channelopathies. *J Am Coll Cardiol*. 2013;62:169–180.
13. Nyegaard M, Overgaard MT, Søndergaard MT, Vranas M, Behr ER, Hildebrandt LL, et al. Mutations in calmodulin cause ventricular tachycardia and sudden cardiac death. *Am J Hum Genet*. 2012;91:703–712.